5-2011

Molecular Modulation of a-Subunit VISIT-DG Sequence Residue Asp-350 in the Catalytic sites of *Escherichia coli* ATP Synthase.

Sneha R. Jonnalagadda
East Tennessee State University

Molecular Modulation of α-Subunit VISIT-DG Sequence Residue Asp-350 in the Catalytic Sites of *Escherichia coli* ATP Synthase

---

A thesis

presented to

the faculty of the Department of the Biological Sciences

East Tennessee State University

In partial fulfillment

of the requirements for the degree

Master of Science in Biology

---

by

Sneha Reddy Jonnalagadda

May 2011

Michael S. Zavada, Ph.D. Chair

Karl Joplin, Ph.D.

Hugh Miller, Ph.D.

Key words: F_1F_o- ATP Synthase, ATP Synthesis, *E. coli*, biological nanomotor, VISIT-DG Sequence, NBD-Cl, Mg-ADP, DTT, Aluminum chloride, Scandium chloride, DCCD.

ABSTRACT

Molecular Modulation of α-Subunit VISIT-DG Sequence Residue Asp-350 in the Catalytic sites of *Escherichia coli* ATP Synthase

by

Sneha Reddy Jonnalagadda

ATP Synthase is the fundamental means of cellular energy production in animals, plants, and almost all microorganisms. In order to understand the mechanism of ATP catalysis, critical amino acid residues involved in Pi binding have to be identified. The αVISIT-DG sequence at the interface of α/β subunits that contains residues from 345-351 is highly conserved and αAsp-350 has been chosen because of its negative charge side chain and its close proximity (~2.8 Å) to the known phosphate binding residue αArg-376. The mutant's αD350R, αD350Q, αD350A, αR376A/D, and αG351R/A/D were generated by site directed mutagenesis and several biochemical assays were performed on them to understand the role played by the amino acid residues in Pi binding. Biochemical results suggest that αD350 may be involved in catalysis of ATP synthase and play an important role in Pi binding, whereas αG351 may be involved only in the structural integrity.

ACKNOWLEDGMENTS

I would like to express my deep and sincere gratitude to my supervisor Dr. Michael S. Zavada for his support throughout this work. I wish to express my warm and sincere thanks to my committee members Dr. Karl Joplin and Dr. Hugh Miller for their detailed and constructive comments. I would like to acknowledge department of biological sciences for providing me financial assistance, without which it would have been impossible for me to do master's abroad.

I owe my loving thanks to my dear husband Rakesh Ponnala for his understanding and encouragement in every step of my career. Finally, I would like to thank my dear family members, friends, and my fellow graduate and undergraduate students for their support.

CONTENTS

LIST OF TABLES

LIST OF FIGURES

CHAPTER 1

INTRODUCTION

ATP synthase, also known as F_1F_o –ATPase, is the fundamental means of energy production that catalyzes the synthesis of ATP during oxidative phosphorylation or photophosphorylation. The enzyme is capable of hydrolyzing and synthesizing ATP in a reversible reaction. The enzyme was discovered in 1929 by Karl Lohmann, and in 1935 Vladimir Engelhart noted that muscle contractions require ATP. Fritz Lipmann demonstrated that ATP is the main bearer of chemical energy in the cell in 1941, and Alexander Todd synthesised ATP chemically in 1948. Slater proposed a scheme showing the chemical intermediates to explain the mechanism of oxidative phosphorylation [1]. Coupled oxidative phosphorylation was shown to be activated by a soluble factor in bacteria particulate [2]. Soluble adenosine triphosphatase was then shown to participate in oxidative phosphorylation [3]. The chemiosmotic hypothesis postulated the primary role of membranes that separate 2 compartments and therefore maintains a gradient of proton activity, generated by respiration chain enzymes, that was used by ATP synthase [4]. On the basis of the kinetics of enzyme-catalysed ^{18}O exchange between H_2O and P_i/ATP, a binding change mechanism was proposed. The binding change mechanism involves the active site of a β subunit cycling between three states. In the "open" state, ADP and phosphate enters the active site where the protein then closes up around the molecules and binds them loosely. The enzyme then undergoes another change in shape and forces these molecules together, with the active site in the resulting tight state binding the newly-produced ATP molecule with very high affinity. The active site then cycles back to the open state, releasing

ATP and binding more ADP and phosphate, ready for the next cycle of ATP production. The F_1 catalytic domain of ATP synthase was crystallized, which essentially supported the hypothesis that Boyer's binding change mechanism was correct.

In view of the fact that ATP synthase uses ATP to drive proton gradient for transport purposes, it is highly conserved in all organisms. In *Escherichia coli*, ATP synthase has 2 major components (F_1 and F_o) and 8 different subunits (α_3, β_3, γ, δ, ε, a, b, $c_{10\text{-}15}$). The water soluble F_1 sector is made up of 3α subunits, 3β subunits and one each of γ, δ, and ε subunits. The membrane embedded F_o sector consists of 1a, 2b and 10-15c subunits [Fig 1]. The overall molecular mass of the complex is ~530KDa.

ATP synthase has 3 catalytic sites located on the α/β interface. Proton pumping occurs through membrane embedded F_0 sector [5, 6]. The F_1 subunit is part of the "rotor" that is composed of γ,ε, and a ring of c subunits. The γ-subunit is comprised of three α-helices. 2 of these helices form a coiled coil that go right up into the central space of the $\alpha_3\beta_3$ hexagon. The "stator" is composed of 2 b and δ subunits. The function of the stator is to prevent co-rotation of catalytic sites and the 'a' subunit with the rotor [7, 8]. Proton gradient-driven clockwise rotation of γ (as viewed from the membrane) leads to ATP synthesis and anticlockwise rotation of γ results in ATP hydrolysis. ATP synthase works like a motor and in fact it is the smallest known biological nanomotor. Detailed reviews of ATP syntheses structure and function may be found in references [9-16].

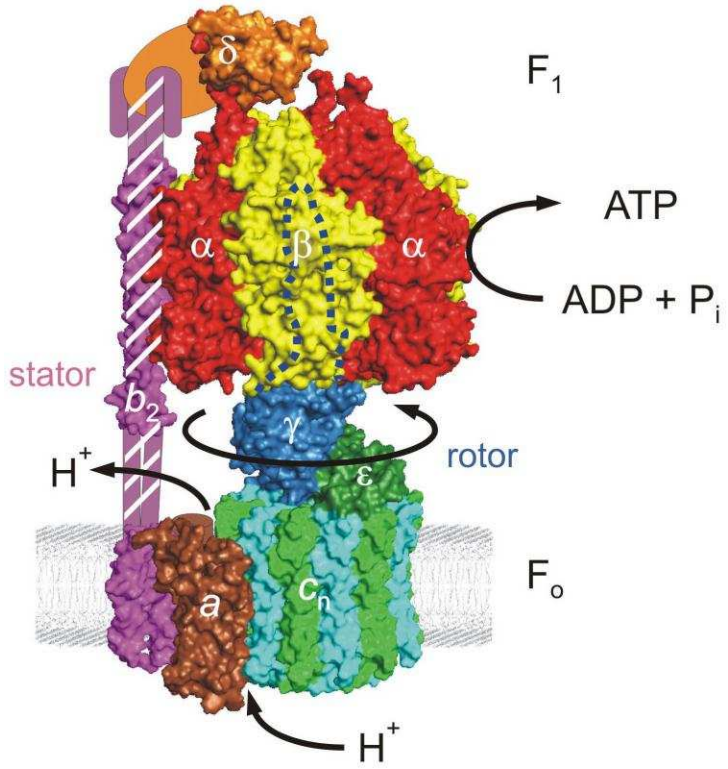

Figure 1: The Rotary Mechanism of ATP Synthase. (Reproduced from [42] with permission; copyright Elsevier).The enzyme consists of 2 sectors catalytic F_1 and membrane bound F_o. F_1 consists of α_3, β_3, γ, δ, and ε. F_o consists of ab_2c_{10}. In mitochondria and chloroplasts additional subunits are present. The rotor stalk indicates the helical coiled-coil extension of the γ subunit into the central cavity of the α_3/β_3 hexagon. The rotor is composed of γ, δ, and a ring of c subunits. The "stator" is composed of b2δ. The proton pathway lies between 'a' and 'c' subunits. [39]

Determining the Reaction Mechanism of ATP Synthase

In order to understand the reaction mechanism of ATP synthesis and hydrolysis and their relationship to rotation in this biological nanomotor, our lab has focused mainly on

- Understanding the role of conserved residues in and around catalytic site Pi-binding sub-domain [22].
- Modulating the catalytic site for improved catalytic and motor function of the enzyme.
- Understanding the relationship between Pi binding and subunit rotation [20-22].
- How ATP synthase binds ADP and Pi within its catalytic sites in the face of relatively high ATP/ADP concentration ratio.

Importance of VISIT-DG

The α-subunit Valine, Isoleucine, Serine, Isoleucine, Threonine, Aspartate, Glycine (VISIT-DG) [Fig 2] residues are highly conserved throughout all living organisms. Earlier αArg-376, βArg-182, βLys-155, and βArg-246 were shown to be involved in Pi binding [20, 22]. Recently αSer-347 of VISIT-DG sequence was also indentified as a fifth Pi binding residue [22, Fig 3]. Generally, the other VISIT-DG sequence residues are of special interest and in particular, αAsp-350 is of special interest due to its negative charge. This residue is also in close proximity (~2Å) to αArg-376, a known Pi binding residue. Here, we would like to investigate the role of αAsp-350 in direct/ indirect Pi binding and or in the maintenance of the Pi binding subdomain.

```
E. coli          RAARVNAEYVEAFTKGEVKGKTGSLTALPIIETQAGDVSAFVPTNVISITDGQIFLETNL
B. taurus        RAAKMNDAF----------GGGSLTALPVIETQAGDVSAYIPTNVISITDGQIFLETEL
H. sapiens       RAAKMNDAF----------GGGSLTALPVIETQAGDVSAYIPTNVISITDGQIFLETEL
P. abelii        RAAKMNDAF----------GGGSLTALPVIETQAGDVSAYIPTNVISITDGQIFLETEL
D. rerio         RAAKMNDNF----------GGGSLTALPVIETQAGDVSAYIPTNVISITDGQIFLETEL
R. norvegic      RAAKMNDSF----------GGGSLTALPVIETQAGDVSAYIPTNVISITDGQIFLETEL
S. salar         RAAKMNENF----------GGGSLTALPVIETQAGDVSAYIPTNVISITDGQIFLETEL
G. gallus        RAAKMNDSF----------GGGSLTALPAIETQAGDVSAYIPTNVISITDGQIFLETEL
X. Tropical      RAAKMNDHF----------GGGSLTALPVIETQAGDVSAYIPTNVISITDGQIFLETEL
A. aegypti       RAAKMNPTL----------GGGSLTALPVIETQAGDVSAYIPTNVISITDGQIFLETEL
B. mori          RAAKMSDKM----------GGGSLTALPVIETQAGDVSAYIPTNVISITDGQIFLETEL
B. malayi        RAAKMNDSH----------GGGSLTALPVIETQAGDVSAYIPTNVISITDGQIFLETEL
P. fucata        RAAKMNDDN----------GGGSLTALPVIETQAGDVSAYIPTNVISITDGQIFLETEL
S. purpurat      RAAKMNPDF----------GGGSLTALPVIETQAGDVSAYIPTNVISITDGQIFLETEL
C. intestin      RAAKMSDAF----------GGGSLTALPVIETQAGDVSAYIPTNVISITDGQIFLETEL
H. mealybug      RAAKMNEKE----------GGGSLTALPVIETQAGDVSAYIPTNVISITDGQIFLETEL
A. fumigatu      RAAKMNDKH----------GGGSLTALPVIETQGGDVSAYIPTNVISITDGQIFLESEL
P. marneffe      RAAKLNDKH----------GGGSLTALPVIETQGGDVSAYIPTNVISITDGQIFLETEL
S. cerevisiae    RAAKLSEKE----------GSGSLTALPVIETQGGDVSAYIPTNVISITDGQIFLEAEL
```

Figure 2: Amino Acid Sequence Alignment of Evolutionarily Conserved α-subunit VISIT-DG Sequence. (Adapted from [22] with permission from ASBMB, 2009) α- subunit sequence from different species is aligned. The highly conserved VISIT-DG sequence is highlighted in *gray*. The starting residue arginine shown here for *E. coli is* αR300. [22]

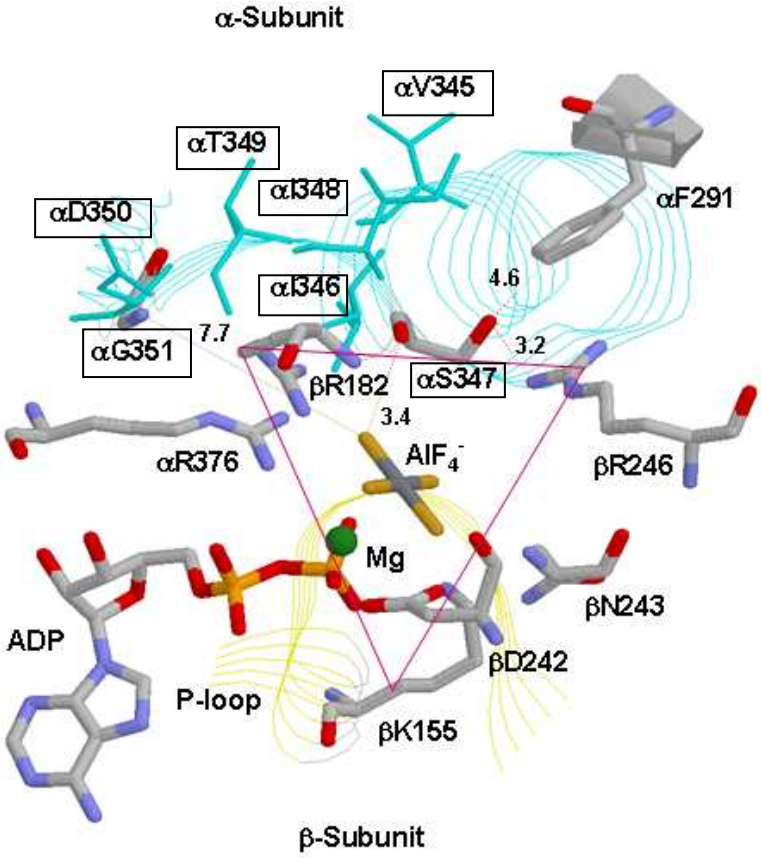

Figure 3: X-Ray Crystal Structure of Catalytic Sites in the α-subunit of Mitochondrial ATP Synthase. (Adapted from [22] with permission from ASBMB, 2009) The triangle showing the residues βR182, βK155, αR376, βR246, αS347 together form a catalytic triad. αD350 is of special interest due to its close proximity (~2A^{o}) to a known Pi binding residue αR376.Residues in the boxes define the VISIT-DG. [22]

Inhibition of ATP Synthase

7-chloro-4-nitrobenzo-2-oxa-1, 3-diazole (NBD-Cl) is a potent inhibitor of ATP synthase. It provides a measure of the Pi binding. NBD-Cl reacts with the phenolic oxygen of Tyr-311 of the βE subunit that contains no bound nucleotide. The 2 other catalytic subunits βTP and βDP contain bound adenylyl-imidodiphosphate (AMP-PNP) and ADP respectively. The binding site of the NBD moiety doesn't overlap with the regions of βE that form the nucleotide binding pocket in subunits βTP and βDP, nor does it occlude the nucleotide-binding site. Catalysis appears to be inhibited because neither βTP nor βDP can accommodate a Tyr-311 residue bearing a NBD group. NBD-Cl inhibits the enzyme by preventing the modified subunit from adopting a confirmation that is essential for catalysis to proceed. NBD-Cl forms a covalent adducts with βTyr-297 in E.*coli* at a stoichiometry of 1mol/mol and inhibits F_1 ATPase activity [17]. NBD-Cl reacts only in the empty (βE) catalytic site, and it doesn't act as a nucleotide analog based on the location of the derivatized Tyr residue in the X-ray structure.

This was supported by the 2 lines of evidence. Pseudo-first order rate constant for inhibition (K_{Obs}) was linearly dependent upon NBD-Cl concentration, implying that no initial binding event was required. Secondly, MgADP protected purified F_1 and F_1F_o in membrane from reaction with NBD-Cl, but only at extremely high concentration that would effectively keep the third site (βE) occupied in time average and thus impede access by NBD-Cl by closing the site [17]. Eventually Perez *et* al. [18] reported that Pi protection against NBD-Cl inhibition of ATPase activity of ATP synthase in mitochondrial membrane preparations, potentially a tool to assay Pi binding in βE catalytic site. This was applicable to both membrane bound enzyme and with purified F_1 from *E. coli* [9]. Several inhibitory studies were performed using transition state analogs. The transition state analog MgADP-AlF_4^- trapped in catalytic sites has been visualized

by x-ray crystallography [19], and it is clear that the fluoroaluminate group occupies the position of phosphate in the transition state complex can be compared by assay of inhibition of ATPase activity by MgADP-fluoroaluminate (MgADP-fluoroscandium) in mutant and wild-type enzymes [20, 21].

Hypotheses

- The highly conserved α-subunit VISIT-DG sequence residue Asp-350 is directly or indirectly involved in phosphate binding through αArg-376.
- αAsp-350 is important for function through its role in maintaining the structural integrity of the Pi binding subdomain and not involved in Pi binding per se.
- The carboxyl side chain of αAsp-350 may be involved in establishing transition state.
- The compensatory effect of αD350 can be determined through αD350R/αR376A and repulsive effect through αD350/αR376D [13]. This can help in exploring the role of αD350 in Pi binding and/or structural integrity.

The aspartate and glycine residues of VISIT –DG sequence have been replaced by various other amino acids such as arginine, glutamine, alanine, etc through site directed mutagenesis. Left and right oligonucleotides were designed with the desired mutations. The single stranded template DNA was amplified in PCR using DNA polymerase and primers. These plasmids, thus obtained, were then transformed into the DK8 strain that lacks ATP synthase gene. The plasmids isolated from DK8 were then sent to sequencing to confirm the presence of desired mutations. Once the desired mutants are obtained, several inhibitory studies were carried on the membranes of different mutants. These inhibitory studies enable us to understand the role played by different residues in phosphate binding.

CHAPTER 2

MATERIALS AND METHODS

Chemicals

Adenosine 5□-triphosphatase disodium salt, ampicillin, glucose, succinic acid, uracil, TES, TRIZMA (Tris[Hydroxyethyl] ethane), 4-aminobenzamidine dihydrchloride (PAB), SDS (Sodium dodecyl sulfate), Isopropyl β-D-1-thiogalactopyranoside (IPTG), 5-bromo-4-chloro-3-indolyl- beta-D-galactopyranoside (X-Gal), βmercaptoethanol, agarose, adenosine 5'-diphosphate (ADP), 4-chloro-7-nitrobenzofurazan (NBD-Cl) , *N,N′*-dicyclohexylcarbodiimide (DCCD), dithiothreitol **(**DTT), sodium fluoride (NaF), aluminum chloride($AlCl_3$), and scandium chloride($SnCl_3$) were purchased from Sigma–Aldrich Chemical Company.

Buffers and Reagents

50mM Tris-H_2SO_4 (pH-8), ATPase assay buffer, T&S reagent (Taussky and Shorr reagent), 10%SDS, TE(trace elements), 1M MgSO4, AET (Arginine Ent Thiamine), ILV(isoleucin-valine), STEM, TES 50, and TES5 +PAB, 10x reaction buffer, dNTP mix, quick solution reagent, cell resuspension solution, column wash solution, and neutralization solution were prepared as described in Appendix B.

Culture Media

LB medium, minimal media, limiting glucose, succinate media, NZY broth, XL ultra competent cells, and culture media (liquid and plates) were prepared as described in Appendix C.

All other standard chemicals used in this study were ultra pure analytical grade purchased either from Sigma-Aldrich Chemical Company or Fisher Scientific Company.

Equipment

Table top centrifuge (Thermo Scientific), Polymerase chain reactor, Gel doc, Stasar III Colorimeter (Gilford, Oberlin, OH) Evolution-300 UV-Visible Spectrophotometer (Thermo Scientific, Pittsford, NY), French press, cell disrupter (Thermo Scientific, Asheville, NC), C76 Water Bath shaker (New Brunswick Scientific Co. inc, Edison, NJ), Sorvall WX ultra 80, Ultra Centrifuge (Thermo Scientific, Asheville, NC), Sorvall RC-5Bsuper speed Centrifuge (Thermo Scientific, Asheville, NC), Series 25, and incubator shaker (New Brunswick Scientific Co. inc, Edison, NJ) were used during experiments.

Designing the Primers

The mutagenic primers must contain the desired mutations and anneal to the same sequence on the opposite strand of the plasmid. The primers were designed with a minimum GC content of 40% and approximately of 25 to 45 bases in length with a Tm>78°C. The desired mutation was in the middle of the primer with ~10-15 bases of correct sequence on both sides.

Site-Directed Mutagenesis

Mutagenesis was performed using Quick-change site directed mutagenesis kit [26]. In site directed mutagenesis a super coiled double stranded DNA vector (M13mp18) with an insert of interest (α-subunit of E. coli ATP synthase) has been used. The left and right oligonucleotides were synthesized with the desired mutation and were used during reaction. The left and right

primers, each complementary to the vector, are extended in a polymerase chain reaction by DNA polymerase. Thus, the mutant plasmids with the nicks were generated. These nicks were cleaved by DpnI endonucleases and the nicked mutated plasmid DNA was transformed into XL1-supercompetent cells. The plasmids from these mutants were isolated and transformed into DK8 strains that lack ATP synthase gene. The reaction procedure is described as below.

The control reaction was prepared using 10x Reaction buffer, 10ng of pBW4.5kb control plasmid (5ng/µl), 125ng of oligo control primer1 [34mer (100ng/µl)], 125ng of oligo control primer2 [34mer (100ng/µl)], 1µl of dNTP mix, and 3µl of quick solution reagent. The final volume was made to 50µl using water. The sample reaction was prepared using 5µl of 10x reaction buffer, 10-100ng of dsDNA template, 125ng of oligo primer1, 125ng of oligo primer2, 1µl of dNTP mix, and 3µl of quick solution reagent. Final volume was made to 50µl using water. 1µl (2.5U/µl) of quick change lightning enzyme (DNA polymerase) was added to each of the control and sample reactions. The cycling parameters for PCR are shown in Table 1.

Table1: Cycling Parameters for the Polymerase Chain Reaction

Segment	Cycle	Temperature	Time
1	1	95°C	2min
2	18	95°C, 60°C, 68°C	20sec,10sec,30sec/kb
3	1	68°C	5min

Once the PCR was done, DpnI restriction enzyme was added to each of the vials [26]. The reactions were incubated for 1 hour to digest the parental (i.e: the nonmutated) super coiled dsDNA. In order to transform, XL10 ultra competent cells were used. 45µl of ultra competent cells were aliquoted and mixed with 2µl of βmercaptoethanol to improve transformation

efficiencies. The mixture was incubated on ice for 10 minutes. 2µl of DpnI treated DNA from control and sample reactions were transferred into separate aliquots of ultra competent cells and incubated on ice for 30 minutes. The tubes were given heat pulse for about 30 seconds and immediately placed on ice for 2 minutes. 0.5ml of NZY broth was added to each tube and allowed it to incubate at 37°C for 1 hour with shaking at 225-250 rpm. Cells were spread on LB-AMP agar plates containing 80µg/µl X-Gal and 20mM IPTG, and the plates were incubated at 37°C for more than 16 hrs. Once the positive colonies were observed, they are picked and grown in LB-AMP broth for 6-8 hrs. The plasmids were isolated using Promega mini prep kit.

Plasmid Isolation

10ml (low-copy-number plasmid) of bacterial culture was harvested by centrifugation for 5 minutes at 10,000 x *g* in a tabletop centrifuge. The supernatant was discarded and the tubes were inverted to remove the excess media. 250µl of cell resuspension solution was added, and the cell pellet was thoroughly resuspended by pipetting. 250µl of cell lysis solution was added, and mixed by inverting the tube 4 times. The tubes were incubated for 1-5minutes until the cell suspension is cleared. 10µl of alkaline protease solution was added and mixed by inverting the tubes 4 times and were incubated for 5 minutes at room temperature. Alkaline protease inactivates endonucleases and other proteins released during the lysis of the bacterial cells that can adversely affect the quality of the isolated DNA. The incubation should not exceed for more than 5 minutes with alkaline protease solution, as nicking of the plasmid DNA may occur. 350µl of neutralization solution was added and mixed immediately by inverting the tubes 4 times. The lysate was centrifuged at maximum speed (around 14,000 × *g*) in a micro centrifuge for 10 minutes at room temperature. The cleared lysate was transferred to the spin column by decanting.

The supernatant was centrifuged at maximum speed in a micro centrifuge for 1 minute at room temperature and the spin column was removed from the tube, and flow through was discarded from the collection tube. To the spin column, 750µl of column wash solution was added and centrifuged at maximum speed for 1 minute. The supernatant was discarded and again washed with column wash solution by centrifuging at maximum speed for 1minute. The spin column was transferred to a new, sterile 1.5ml micro centrifuge tube.100µl of nuclease-free water was added to the spin column and centrifuged to elute the plasmid DNA. Plasmid DNA was stored at –20°C or below in water.

Once the plasmids were isolated, restriction digestion was performed with specific enzymes for each mutation. The bands were observed on 1% agarose gel electrophoresis using standard protocol. Once the bands of required length are obtained, the plasmids were sent to sequencing. Sequencing results confirmed the presence of mutation and the plasmids with the desired mutation were again transformed into DK8 strain using electroporation method [23, 24]. The mutants were thus obtained and can be used for further experiments.

Growth Yield on Succinate and in Limiting Glucose [28]

The colonies of each mutant strain were streaked on to succinate plates and were observed for 3 days. The mutant strains were inoculated into limiting glucose and allowed to grow at 37°C, 250 rpm in water bath. The O.D was observed at 595nm for every hour till late log phase. This determines the amount of the membrane to be used and time of incubation.

Preparation of *E. coli* Membrane Bound ATP Synthase [27]

Starter Culture

Minimal media was prepared in one large batch and distributed into 250ml flasks with 50ml each for better aeration. Necessary additions were made and the flasks were inoculated with 10-15ml LB-AMP broth that has been previously grown overnight (16-20hrs) at 37°C, 250 rpm and allowed to grow for 6-8 hrs in 37°C water/air shaker at 250 rpm. These were used as inoculums for 1litre flasks.

Bacterial Growth

50ml of overnight starter cultures were inoculated into 1litre minimal media and grown at 37°C, 250 rpm. Growth yield was measured at $O.D_{595}$ every hour till late log phase. Once the late log phase was obtained, the cells were harvested.

Harvesting the Cells

The cells were harvested by spinning the culture at 2°C in a Sorvall RC-5B refrigerated Super speed centrifuge at 9500 rpm for 15 min. The harvested sample was resuspended in STEM and centrifuged at 9500 rpm for 25 min. The supernatant was discarded and the pellet is resuspended in 2 ml STEM/g wet cells and was stored at -80°C overnight.

Membrane Bound ATP Synthase Isolation

Cells from overnight were thawed and mixed with DNAse to digest nucleic acids. The cells were then disrupted by 2 passages through chilled French press cell fractionator at 2000 psi. Cell debris was pelleted by centrifugation at 18K rpm for 20 min using Sorvall WX ultra-80,

Ultra Centrifuge. Subsequently, the membranes were pelleted by spinning the supernatant at 60K rpm for 120 min. The membrane was then resuspended in TES 50 and centrifuged at 60K rpm for 120 min. The pellet was then washed with TES 5 + PAB by spinning twice at 60K rpm for 90 min. Finally the purified membrane was resuspended in 50mM Tris Sulfate (pH 8), 2.5mM $MgSO_4$ and stored at -80°C.

Membrane Concentration and ATPase Assay

Membrane concentrations were found by plotting the absorbance at 595nm using Bradford reagent against standard BSA curve. Amount of membrane and time of incubation depends on growth assays and vary with each preparation. ATPase activity was measured by adding 1 ml of assay buffer containing 10mM NaATP, 4mM $MgCl_2$, 50mM $TrisSO_4$(pH 8) to the purified F_1 or membranes at 37°C and stopped by addition of SDS to 3.3% final concentration. Pi release was assayed by adding 1 ml of T&S reagent containing 10mM (NH4)6Mo7O24·4H2O , 250mM Fe(NH4)2(SO4)2·6H2O, and 1.176 N H2SO4 [29]. The color that developed was measured using a Stasar III Colorimeter at 700 nm. A graph is plotted using Sigma plot software with activity on X-axis and OD_{700} on Y-axis. There is a straight line relationship between the calorimetric reading and the concentration of phosphate. The reaction is:

$$\text{ATP + ATP Synthase} \rightleftharpoons \text{ADP + Pi}$$

$$\text{Pi + T\&S} \longrightarrow \text{Blue color measured at O.D}_{700}$$

Specific Activity= (Sample O.D- Blank O.D) / [Amount (mg)*Time (min)]

Inhibition of ATPase Activity by NBD-Cl

The three catalytic sites located on the F_1 sector of ATPase are βTP, βDP, βE. Pi are supposed to bind in the βE site for ATP synthesis. Fortuitously, NBD-Cl reacts specifically in the βE site thus preventing the ATP synthesis [17]. NBD-Cl reacts with NBD-Cl was prepared as a stock solution in dimethyl sulfoxide and protected from light. The membranes were reacted with different concentrations of NBD-Cl for 60min in dark at room temperature in 50mM Tris-SO_4 (pH 8), 2.5mM $MgSO_4$. Then, 1ml of ATPase assay buffer was added into the tubes and allowed to incubate at varied times for different mutants. The reaction was stopped by 10%SDS and ATPase activity was determined after adding T&S at $O.D_{700}$

- 50mM T8 + Mbr + 150 µM NBD-Cl (inc 1h) + ATP_{cktl} + 10% SDS +T&S (2-5 min)
- 50mM T8 + Mbr + 150 µM NBD-Cl (inc 1h) + 10% SDS +T&S (2-5 min)

Extra Pulse of NBD-Cl

It was mainly performed to see whether the maximal reaction with NBD-Cl occurred or not. The membrane was incubated in dark with 150µM NBD-Cl for 60min at room temperature in 50mM Tris-SO_4, 2.5mM $MgSO_4$, and then, an extra pulse of 200µM NBD-Cl was added and incubated for another 60min. Then, 1ml of ATPase assay buffer was added into the tubes and allowed to incubate at varied timings for different mutants. The reaction was stopped by 10%SDS and ATPase activity was determined after adding T&S at $O.D_{700}$

- 50mM T8 + Mbr + 150 µM NBD-Cl (inc 1h) + 200µM NBD-Cl (inc 1h) + ATP_{cktl} + 10% SDS +T&S (2-5 min).
- 50mM T8 + Mbr + 150 µM NBD-Cl (inc 1h) + 200µM NBD-Cl (inc 1h) + 10% SDS + ATP_{cktl} + T&S (2-5 min).

DTT Reversibility

NBD-Cl inhibition was reversed by incubating the membranes with DTT for 60min at room temperature. NBD-Cl incubations are performed in the dark where as DTT should be maintained cool. The control samples without NBD-Cl and/or DTT were incubated for the same times. Then, 1ml of ATPase assay buffer was added into the tubes and allowed to incubate at varied timings for different mutants. The reaction was stopped by 10%SDS and ATPase activity was determined after adding T&S at $O.D_{700.}$

- 50mM T8 + Mbr + ATP_{cktl} + 10% SDS + T&S (2-5 min)
- 50mM T8 + Mbr + 150 µM NBD-Cl (inc 1h) + ATP_{cktl} + 10% SDS + T&S (2-5 min)
- 50mM T8 + Mbr + 150 µM NBD-Cl (inc 1h) + 4mM DTT (inc 1h) + ATP_{cktl} + 10% SDS + T&S (2-5 min)
- 50mM T8 + Mbr + 4mM DTT (inc 1h) + ATP_{cktl} + 10% SDS + T&S (2-5 min)

Mg Pi Protection Against NBD-Cl

The membranes were preincubated for 60min with Pi and an equimolar Mg^{+2} at room temperature in 50mM Tris-SO_4, 2.5mM $MgSO_4$. The concentration of Pi ranged from 25mM to 100mM. 150µM NBD-Cl was added to the above tubes and incubated at room temperature in the dark for 60min.The control contained the protecting agent without NBD-Cl. Then, 1ml of ATPase assay buffer was added into the tubes and allowed to incubate at varied timings for different mutants. The reaction was stopped by 10%SDS and ATPase activity was determined after adding T&S at $O.D_{700}$

MgADP Protection Against NBD-Cl

The membrane was incubated with MgADP with varied concentrations ranging from 0-12mM before adding NBD-Cl. The concentrations of Mg and ADP should be in 1:1 ratio. Then, 150μM NBD-Cl was added to it and incubated at room temp in the dark for 60min. The control contained MgADP without NBD-Cl and MgADP alone has no inhibitory effect. Then, 1ml of ATPase assay buffer was added into the tubes and allowed to incubate at varied timings for different mutants. The reaction was stopped by 10%SDS and ATPase activity was determined after adding T&S at $O.D_{700}$

Inhibition of ATPase Activity by Transition State Analogs

The membranes were incubated for 60 min at room temperature in 50mM $TrisSO_4$, 2.5mM $MgSO_4$, 1mM NaADP, and 10mM NaF at a protein concentration of 0.2–0.5 mg/ml in presence of $AlCl_3$ or $ScCl_3$ added at varied concentrations. 50μl aliquots were then added to 1 ml of ATPase assay buffer, and activity was measured at $O.D_{700}$. It was confirmed in control experiments that no inhibition was seen if $MgSO_4$, NaADP, or NaF was omitted.

CHAPTER 3

RESULTS

Designing the Mutations and the Enzymes Used to Identify the Mutation

The site directed mutagenesis was performed and the mutants were obtained. The αAsp-350 was mutated to Arginine(R), Glutamine (Q), and Alanine (A). The αArg-376 was mutated to Alanine (A) and Glutamate (D) and the αGly-351 to Arginine (R). The double mutants were also generated to see the repulsive and compensatory effects. The enzymes shown in the Table 2 are used in the restriction digestion of the mutated site. DNA sequencing results confirmed the presence or absence of the mutations.

Table 2: Table Representing the Name, Mutated Site, and Enzymes

Name and Mutated site	Mutation	Enzyme
pSR1 (αD350R)	GAT(D)→CGT(R)	PmlI
pSR2 (αD350Q)	GAT(D)→CAG(Q)	DdeI
pSR3 (αD350A)	GAT(D)→GCG(A)	SacII
pSR4 (αR376A)	CGT(R)→GCC(A)	EagI
pSR5 (αG351R)	GGT(G)→CGT(R)	PvuI
pSR6 (αR376D)	CGT(R)→GAC(D)	AatII
pSR7 (αD350R/ αR376A)	GAT→CGT/CGT→GCC	PmlI-EagI
pSR8 (αD350R/ αR376D)	GAT→CGT/CGT→GAC	PmlI-AatII
pSR9 (αG351R/ αR376A)	GGT→CGT/CGT→GCC	PvuI-EagI
pSR10 (αG351R/ αR376D)	GGT→CGT/CGT→GAC	PvuI-AatII

Growth Yield on Succinate and in Limiting Glucose

A series of mutants were generated. The residue aspartate was chosen for mutagenesis because of its strong conservation in the α-subunit VISIT-DG sequence and its close proximity to the Pi binding pocket. αR376, which is a known Pi binding residue, was also modulated. αD350R /αR376A/D were designed to test the compensatory effect and αD350/αR376D was designed to test the repulsive effect. Table 3 shows that the introduction of arginine and alanine in αD350 and alanine in αR376 resulted in loss of oxidative phosphorylation. Growth yields were very close to null control where as all the double mutants showed partial loss of oxidative phosphorylation. ATPase activities of αD350R, αD350A, αR376A, αG351R are very low when compared to the wild type. However αD350R/αR376A did restore ATPase activity significantly, but the rest of the double mutants are still showing low ATPase activities.

Table 3: Effects of αD350 and αR376 Mutations on Cell Growth and ATPase Activity

Mutation [a]	Growth on Succinate [b]	Growth Yield in Limiting glucose (%)	ATPase Activity [c] (μmol/min/mg)
Wild type	++++	100	11.28
Null	-	52.69	0
(αD350R)	+/-	55	.03
(αD350Q)	++++	65	2.19
(αD350A)	+/-	49	.07
(αR376A)	+/-	56	.06
(αG351R)	+/-	58	.03
(αR376D)	+++	56	.19
(αD350R/ αR376A)	++	73	.46
(αD350R/ αR376D)	+++	68	.04
(αG351R/ αR376A)	+++	61.98	.04
(αG351R/ αR376D)	+++	68	.03

[a] Wild type, pBWU13.4/DK8; Null, PUC118/DK8;
[b] Growth on succinate plates after 3 days estimated by eye. ++++, heavy growth; +, partial growth; +/-, very low growth; -, no growth
[c] ATPase activity was measured at 37°C and expressed as μmol of ATP hydrolyzed/ min/ mg of membrane protein.

Inhibition of ATPase Activity of ATP Synthase by NBD-Cl

NBD-Cl reacts with the phenolic oxygen of Tyr-311 of the βE subunit that contains no bound nucleotide. The 2 other catalytic subunits βTP and βDP contain bound adenylyl-imidodiphosphate (AMP-PNP) and ADP respectively. The binding site of the NBD moiety doesn't overlap with the regions of βE that form the nucleotide binding pocket in subunits βTP and βDP, nor does it occlude the nucleotide-binding site. Catalysis appears to be inhibited because neither βTP nor βDP can accommodate a Tyr-311 residue bearing a NBD group [17].

The NBD-Cl inhibition of each mutant with respect to wild type is shown in Figure 4. Wild type ATP synthase enzyme is shows 100% inhibition, whereas all the newly generated mutants aren't. The αD350Q was almost completely inhibited just like wild type whereas αD350R, αR376D, αD350R/ αR376A, mutants are showing ~80-90% inhibition with 10-20% residual activity. αD350A, αR376A, αG351R/αR376A, αG351R/αR376D mutants are showing 60% inhibition whereas αD350R/αR376D, αG351R are showing 20% inhibition. All the mutants show residual activity. So, in order to see whether NBD-Cl is completely inhibiting the ATP synthase enzyme or not, an extra pulse of NBD-Cl was added.

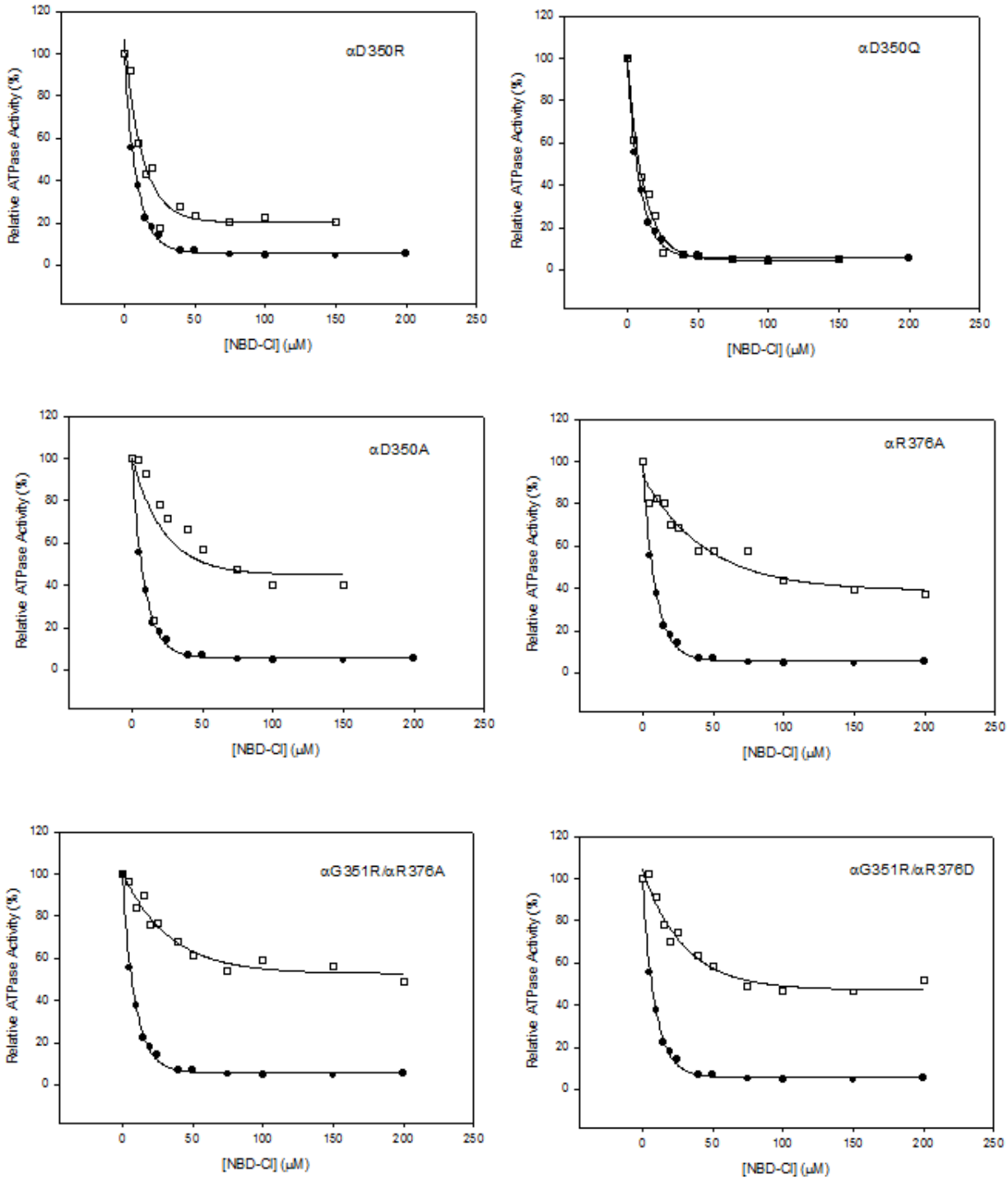

Figure 4: Inhibition of ATPase Activity of Mutants by NBD-Cl. The membranes were preincubated with NBD-Cl for 60 min at RT. The assay was performed as discussed in "Materials and Methods". The solid circles determine wild type and rectangles represent mutants.(Continued on the next page)

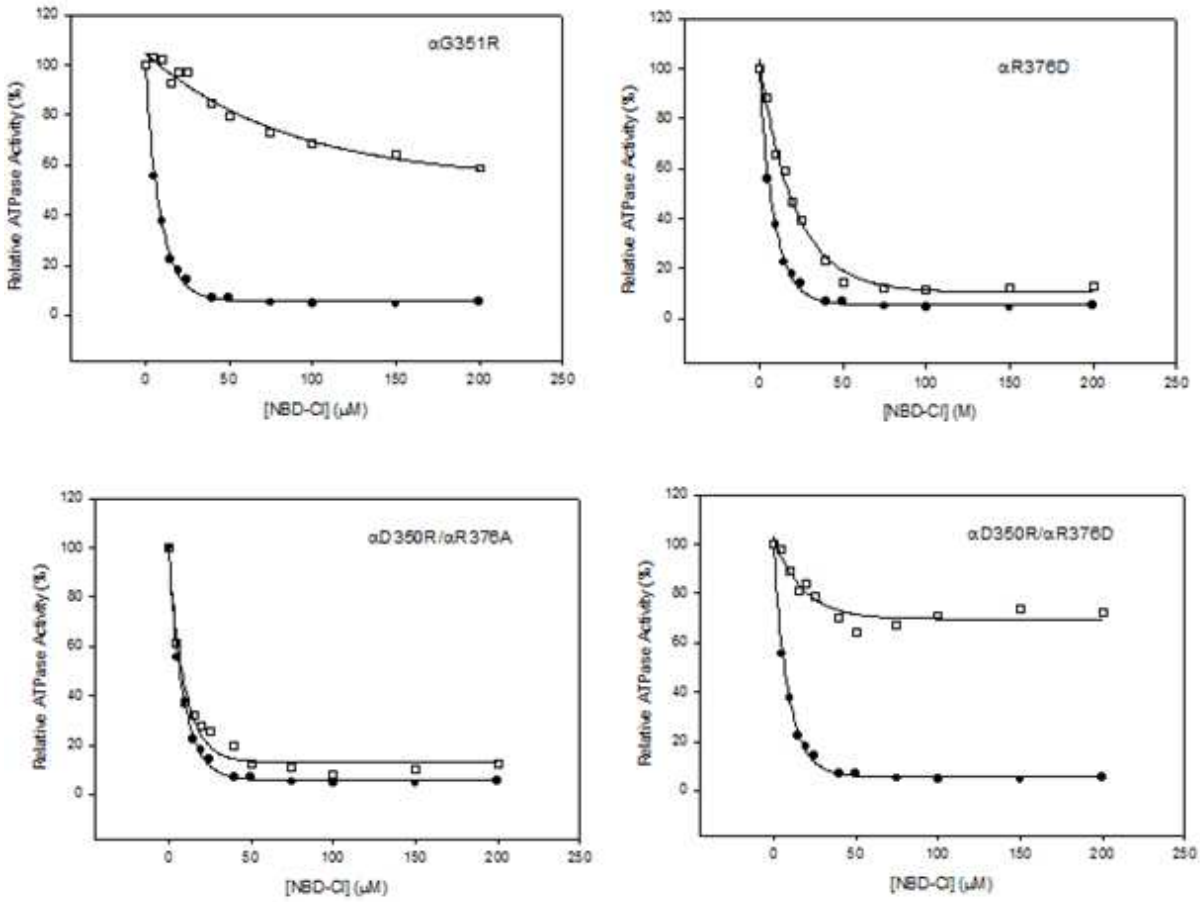

Figure 4: Inhibition of ATPase Activity of Mutants by NBD-Cl. The membranes were preincubated with NBD-Cl for 60 min at RT. The assay was performed as discussed in "Materials and Methods". The solid circles determine wild type and rectangles represent mutants.

Extra Pulse of NBD-Cl

The inhibition with the extra pulse of NBD-Cl was very low. This experiment shows that the NBD-Cl reacts particularly at βE catalytic sites and inhibits the reaction completely. Extra Pulse of NBD-Cl is shown in Figure 5. An extra pulse retained the residual activity.

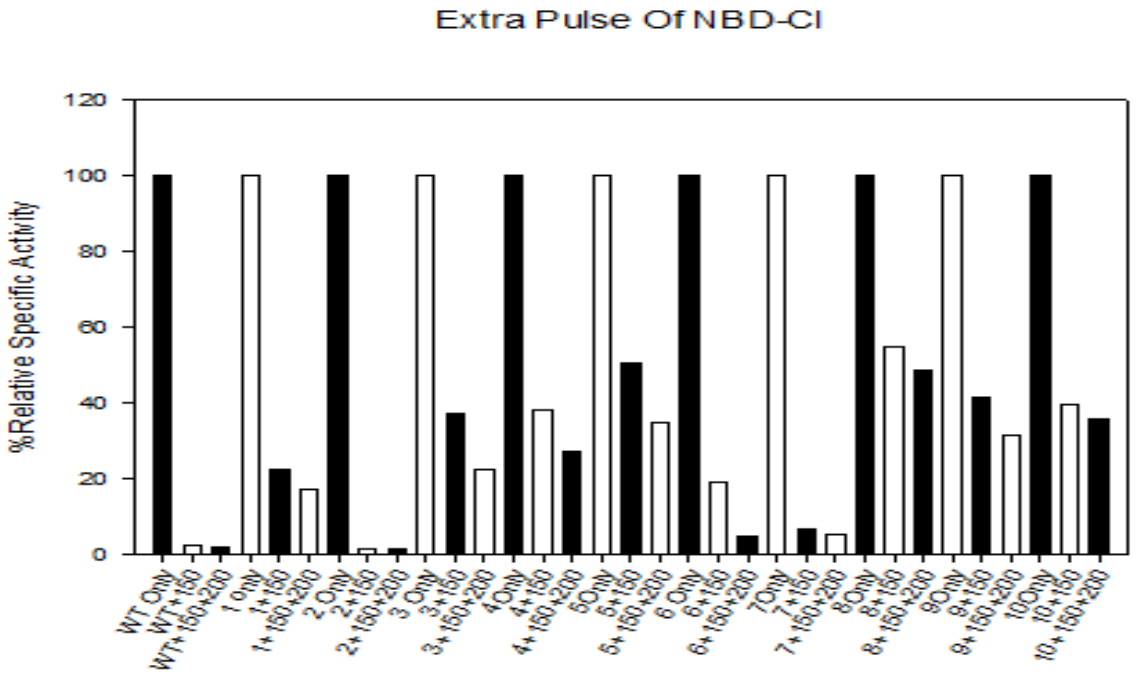

Figure 5: Results of Extra Pulse of NBD-Cl in Mutants: The membranes were incubated for 60min with 150µM NBD-Cl and an extra pulse of 200µM NBD-Cl was added and incubated for another 60min. ATPase assay was performed as described in "Materials and Methods". Each set of bars from represent WT, wild type; 1, αD350R; 2, αD350Q; 3, αD350A; 4, αR376A; 5, αG351R; 6, αR376D; 7, αD350R/αR376A; 8, αD350R/αR376D; 9, αG351R/αR376A;10, αG351R/αR376A from *left* to *right*. The %Relative specific activities of the membranes are: Wild type (100, 2.6, 2.1); αD350R (100, 22.6, 17.9); αD350Q (100,1.4,1.5); αD350A (100,37,22); αR376A (100,38,30); αG351R (100,50,35); αR376D (100,19,10); αD350R/αR376A (100,6,5); αD350R/αR376D (100,56,48); αG351R/αR376A (100,41,31); αG351R/αR376A (100,39,35).

Reversal of ATPase Activity by DTT

DTT assay was performed to see whether the reaction can be completely reversed or not. This assay is an indicative of specificity of reaction. NBD-adduct can be released from βTyr-297, after incubating with DTT [30, 31]. The ATPase activity can be completely regained upon

addition with DTT. The reversal of ATPase activity upon addition with DTT is shown in Figure 6.

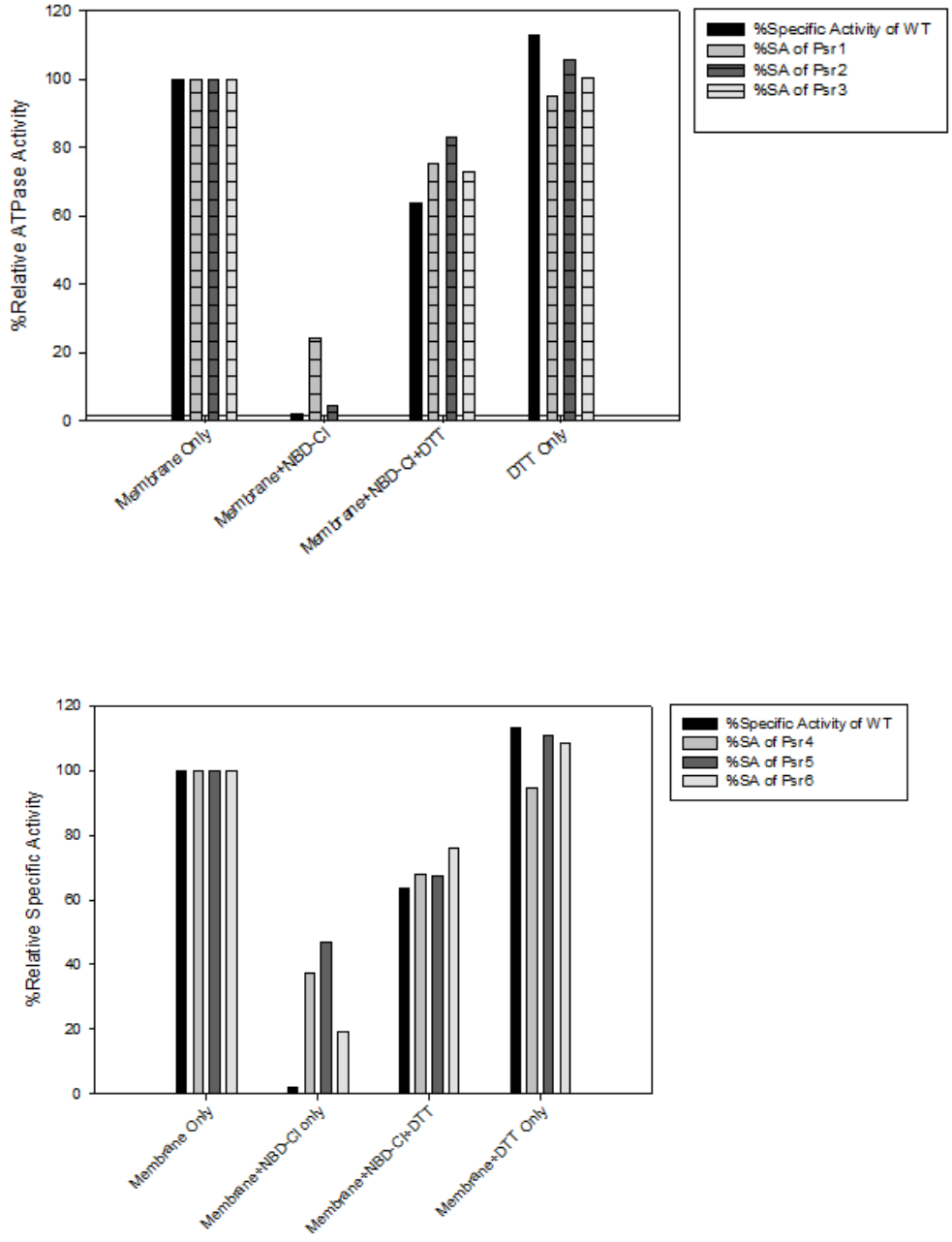

Figure 6: Reversal of ATPase Activity by DTT: Membranes were incubated with NBD-Cl for 60 min, 4mM DTT was added and incubated again for another 60 min. ATPase assay was performed as discussed in "Materials and Methods". Each set of bars on the top figure represent Wild type; psr1, αD350R; psr2, αD350Q; psr3, αD350A from *left* to *right*. Each set of bars in the bottom figure represent Wild type; psr4,αR376A; psr5,αG351R; psr6,αR376D from *left* to *right*.(Continued on the next page)

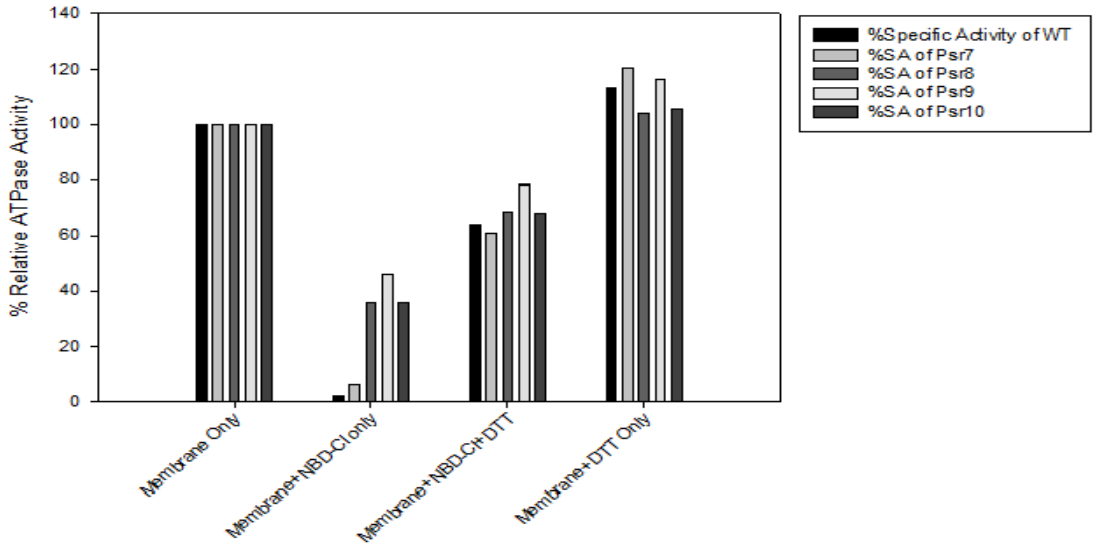

Figure 6: Reversal of ATPase Activity by DTT: Membranes were incubated with NBD-Cl for 60 min, 4mM DTT was added and incubated again for another 60 min. ATPase assay was performed as discussed in "Materials and Methods". Each set of bars represent Wild type; psr7, αD350R/αR376A; psr8, αD350R/αR376D; psr9, αG351R/αR376A; psr10,αG351R/αR376D; from *left* to *right* in each group.

Protection Against NBD-Cl Reaction by MgADP

MgADP protected purified F_1 and F_1F_o in membrane from reaction with NBD-Cl, but only at extremely high concentration that would effectively keep the third site (βE) occupied in time average and thus impede access by NBD-Cl by closing the site [17]. MgADP protection against NBD-Cl inhibition of wild type and mutants is shown in Figure 7.

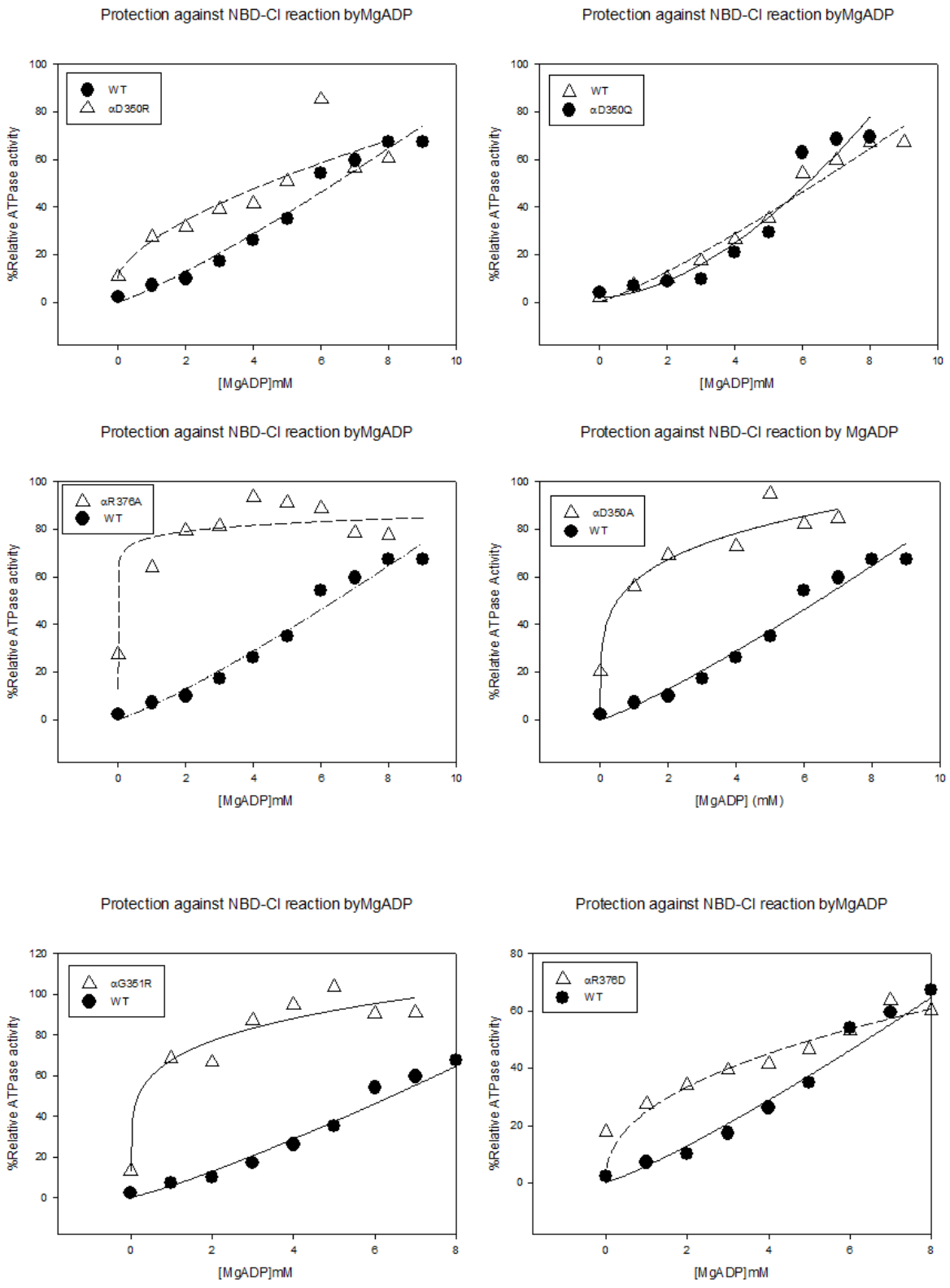

Figure 7: (Continued on the next page)

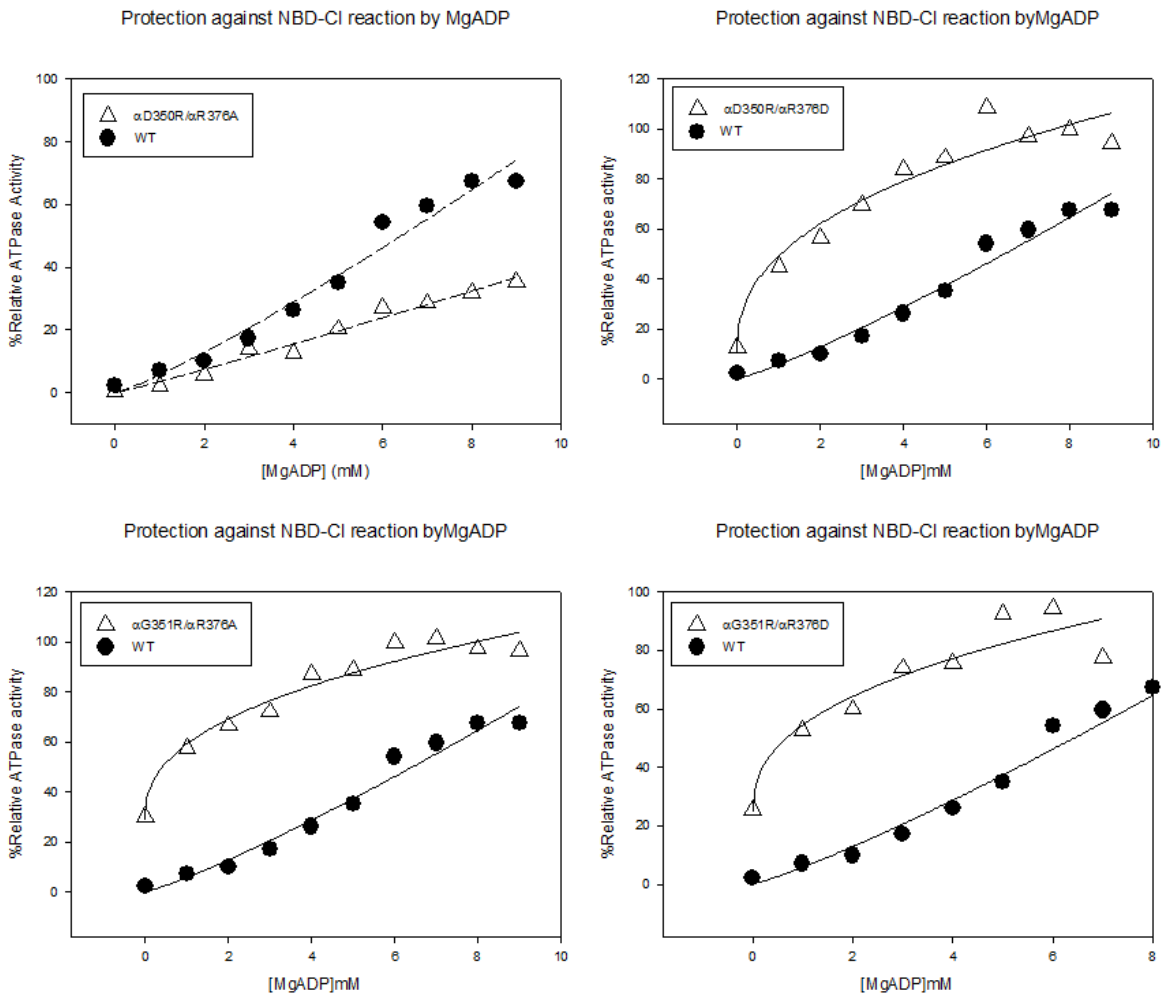

Figure 7: Protection Against NBD-Cl Reaction by MgADP: Wild type and mutant membranes were preincubated for 60 min at RT with varied concentrations of MgADP, then150µM of NBD-Cl was added, and incubation continued at RT in the dark for 60 min. The aliquots were then assayed for ATPase Activity.

Protection by Pi Against NBD-Cl Inhibition

Pi protection against NBD-Cl inhibition of wild type and mutants is shown in Figure 8. Pi protected well against NBD-Cl inhibition of ATPase activity in wild type as well as αD350Q, αD350R, αD350A, αG351R, αR376D, αG351R/αR376A. αD350Q, αD350R, αD350A, αG351R, αR376D, αG351R/αR376A regained Pi binding activity and the introduction of arginine at αG351R compensated the loss of arginine at α376 position.

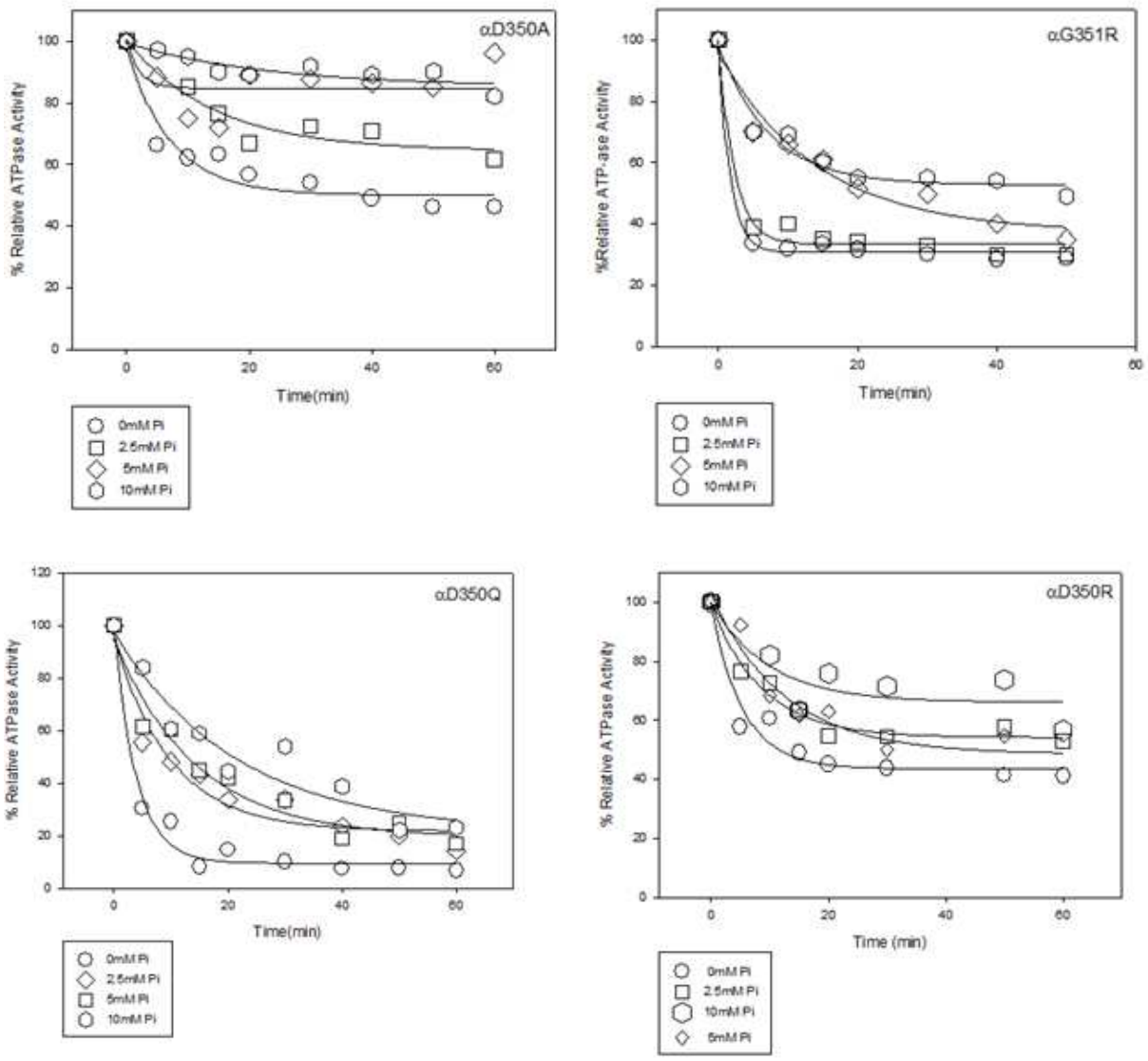

Figure 8: Protection Against NBD-Cl by Pi: Membranes were preincubated with Pi at 0, 2.5, 5, and 10mM concentration as shown, for 60 min at RT. Then NBD-Cl (150μM) was added and aliquots were withdrawn for assay at time intervals. ATPase activity remaining is plotted against time of incubation with NBD-Cl. (Continued on the next page)

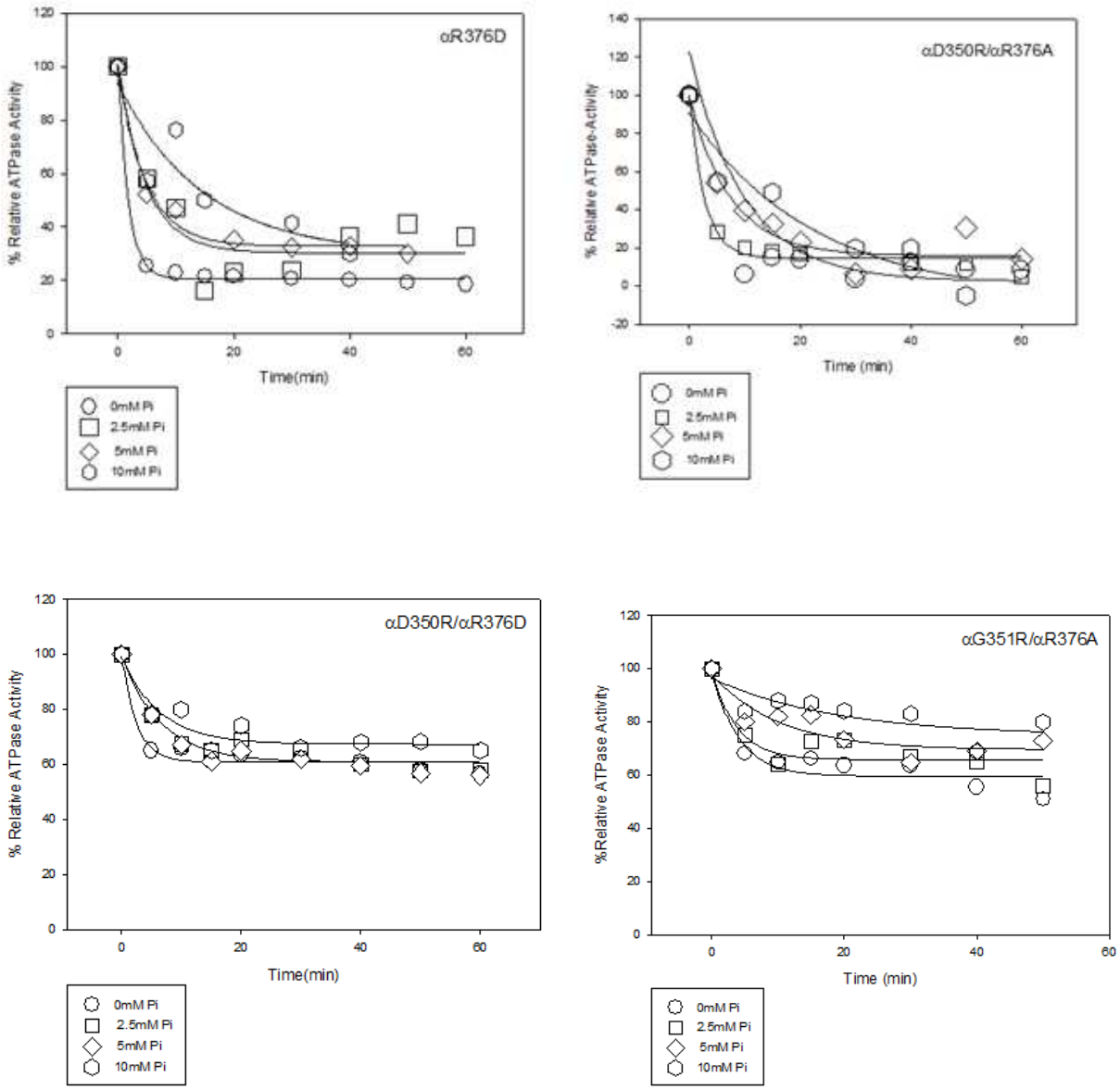

Figure 8: Protection Against NBD-Cl by Pi: Membranes were preincubated with Pi at 0, 2.5,5, and 10mM concentration as shown, for 60 min at RT. Then NBD-Cl (150μM) was added and aliquots were withdrawn for assay at time intervals. ATPase activity remaining is plotted against time of incubation with NBD-Cl. (Continued on the next page)

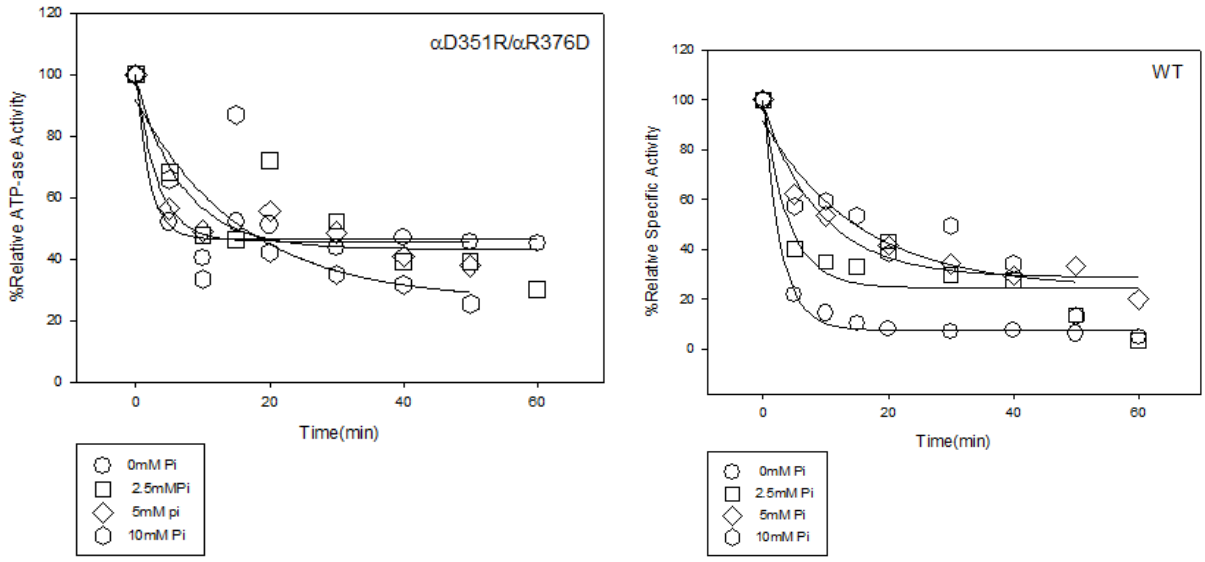

Figure 8: Protection Against NBD-Cl by Pi: Membranes were preincubated with P_i at 0, 2.5, 5and 10mM concentration as shown, for 60 min at RT. Then NBD-Cl (150μM) was added and aliquots are withdrawn for assay at time intervals. ATPase activity remaining is plotted against time of incubation with NBD-Cl.

Inhibition of ATPase Activity by Fluoroaluminate and Fluoroscandium

Inhibition of ATPase activity by transition state analogs is shown in Figure 9. Wild type was strongly inhibited (~>95%) and αD350Q was also strongly inhibited. αR376A was inhibited by 40%, αR376D by 80%, αD350R by 80%, αD350A by 60%, and αG351R by 60%. The introduction of Arginine in αD350R/αR376A resulted in 80% inhibition and αG351R/αR376A and αG351R/αR376D resulted in 40% inhibition. The inhibition of Wild type with fluoroscandium is >98%, αD350Q, αD350R/αR376A by 80%, αG351R by 30%, αR376D by 60%, αD350A by 40%, αD350R/αR376D by 20%, αG351R/αR376D by 10%, and αG351R/αR376A by 30%.

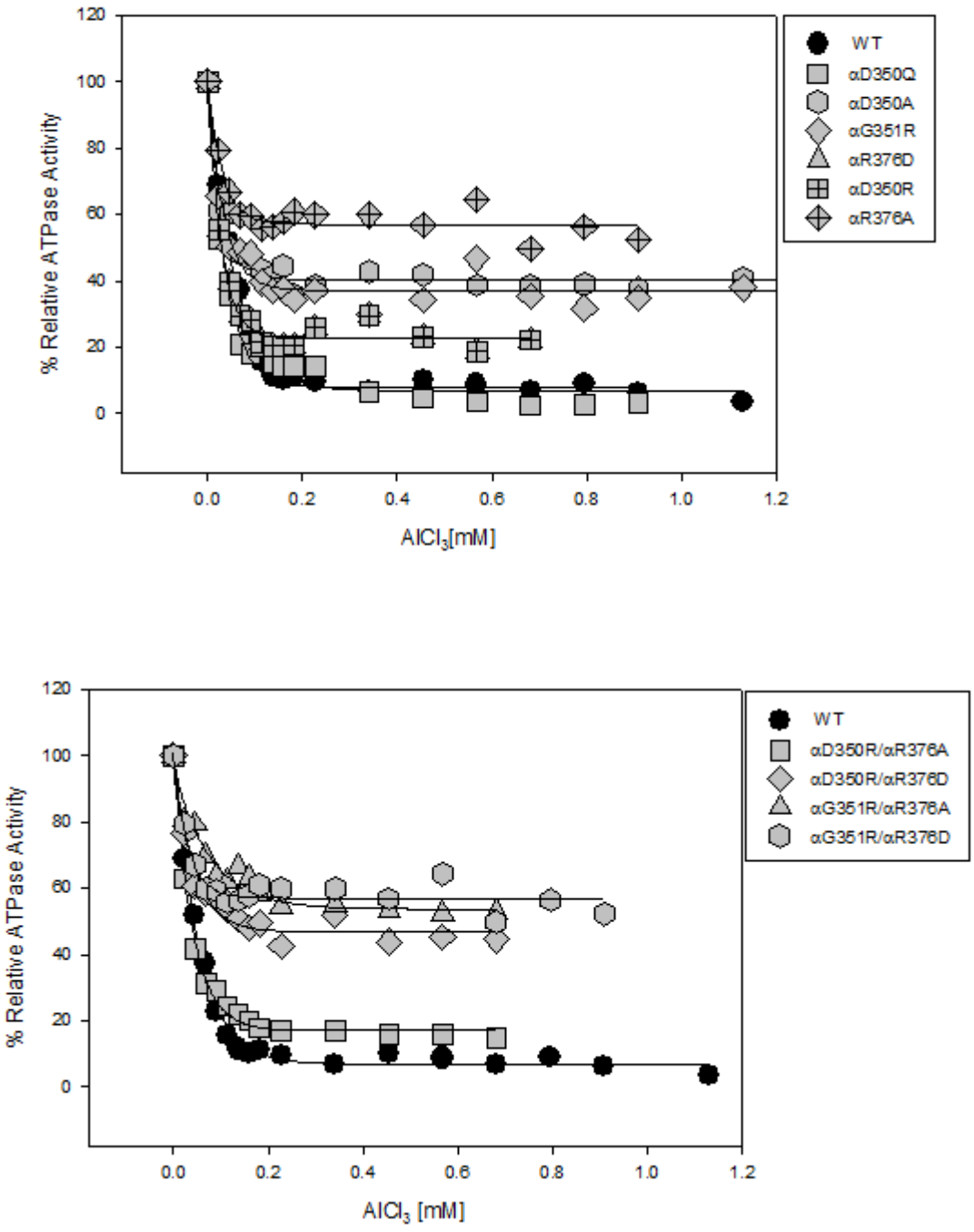

Figure 9: Inhibition of ATPase Activity by Transition State Analogs: The membranes were preincubated for 60 min at room temperature with 1mM MgADP, 10mM NaF, and the indicated concentrations of $AlCl_3$ or $ScCl_3$.Then aliquots were added to 1 ml of assay buffer, and ATPase activity was determined. (Continued on the next page)

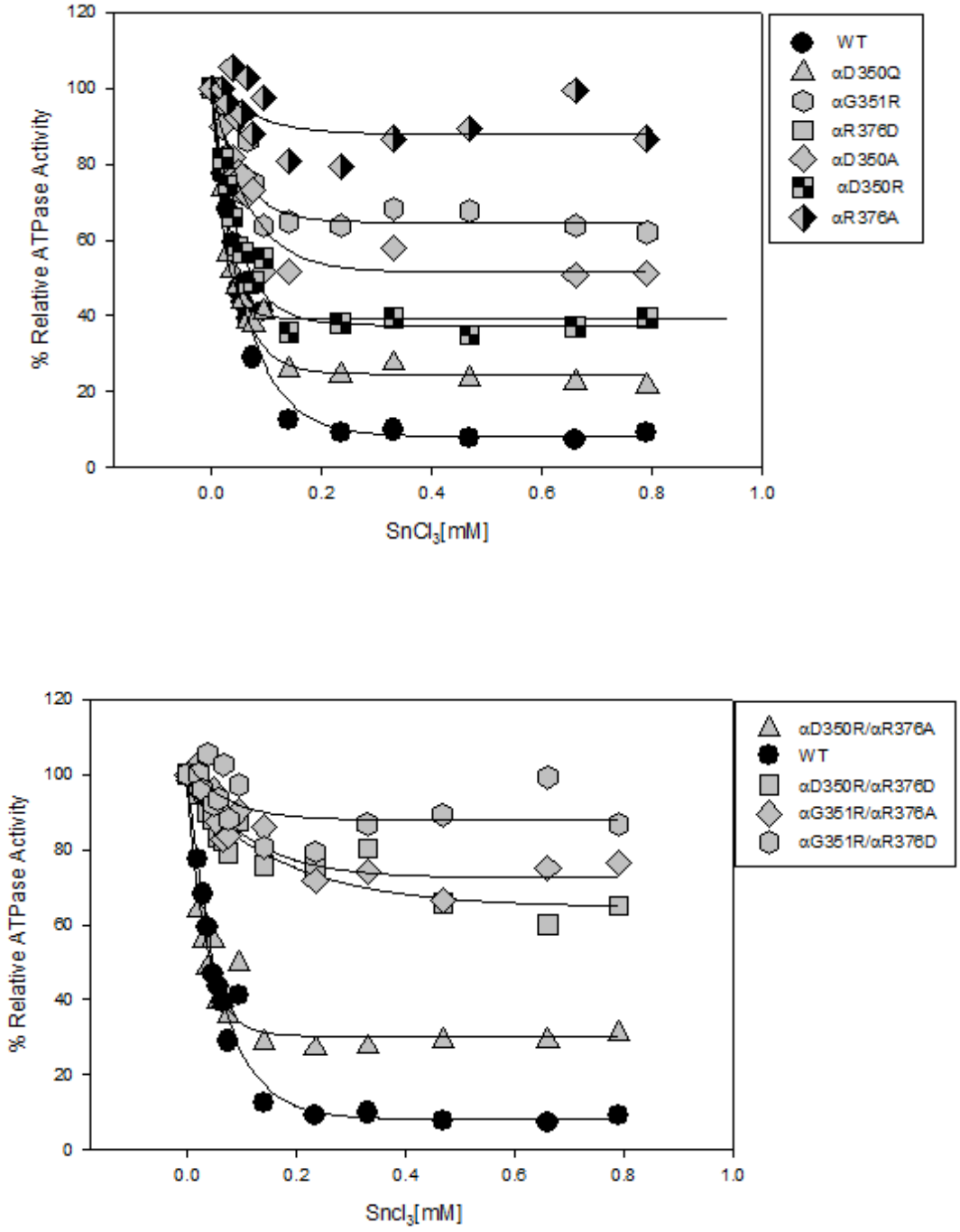

Figure 9: Inhibition of ATPase Activity by Transition State Analogs: The membranes were preincubated for 60 min at room temperature with 1mM MgADP, 10mM NaF, and the indicated concentrations of $AlCl_3$ or $ScCl_3$.Then aliquots were added to 1 ml of assay buffer, and ATPase activity was determined.

CHAPTER 4

DISCUSSION

ATP synthase is one of the smallest known biological nanomotors. ATP synthase exists in the body, interacting with any number of proteins and other molecules at any given time, so why not use this enzyme as a base model to develop a tiny machine that can go inside our bodies to perform various types of work?

Nanomedicine, an offshoot of nanotechnology, refers to highly specific medical interventions on the molecular scale for curing disease or repairing damaged tissues [40]. Unclogging arteries, fighting infections, or helping to monitor body systems are a few things nanomachines might be capable of. But once a nanomachine is inside the body, how big can it be? How fast can it work? Can we alter its speed? How many can we have to perform efficiently without disrupting homeostasis? These questions must be addressed in order to build nanomachines that are compatible with living tissues and can safely operate inside the body [41]. Currently, ATP synthase is the smallest known biological nanomotor. Therefore, understanding the mechanisms of how this enzyme works and using ATP synthase as a base model may help to develop nanomotors for nanomedicine usage.

ATP synthesis occurs by the phosphorylation of ADP. According to binding change mechanism, ADP and phosphate enter the active site where the protein closes up around the molecules and binds them tightly, thus releasing ATP molecule. This process involves several residues and understanding the role of conserved residues in and around catalytic sites is the primary goal of the project. Earlier it was found that positively charged residues are functionally important for Pi binding in the βE catalytic site of *E. coli* ATP Synthase [20]. In certain other

cases [32] introduction of negative charge in the Pi binding pocket close to βArg-246 prevented Pi binding. This gave us an idea to modulate the sites that are very close to the phosphate binding residues and understand the mechanism of phosphate binding. Previously, it was found that αSer-347 of VISIT-DG sequence was involved in Pi binding. The residues αIle-346, αIle-348 and αThr-349 were also modulated to see whether they play an important role in Pi binding or not.

The α-subunit VISIT-DG sequence residue aspartate (D) is ~2.8A^0 from R376 of α-subunit [Fig 2]. The VISIT-DG sequence was chosen because of its conserved nature in many organisms. Here we introduced the mutation αD350R (removal of negative charged side chain and addition of positive charge), αD350Q (addition of bulky group), αD350A (removing charge and size). Here, we mutated the known phosphate binding residue αArg-376 to alanine (A) and tried to see its compensatory effect in αD350R background. We mutated αArg-376 to aspartate(D) in which we removed positive charge side chain and added a negative charge and tried to see the repulsive effect in normal background. The αGly-351 is mutated to arginine (R), a positive charged side chain to see the effect on Pi binding in normal background.

The succinate and limiting glucose assays on the mutants showed partial loss of oxidative phosphorylation and ATPase activities were very low when compared to the wild type [Table 2].

NBD-Cl inhibition assay showed that αD350Q was just like wild type whereas αD350R, αR376D, and αD350R/ αR376A are showing 80-90% inhibition with 10-20% residual activity [Fig 4]. αD350A, αR376A, αG351R/αR376A, αG351R/αR376D showed 60% inhibition compared to wild type [Fig 4].This indicates that NBD-Cl still reacted with βTyr-297 in the mutants as in wild type and an extra pulse of NBD-Cl determined that it reacted particularly in βE catalytic sites and inhibited the reaction completely [Fig 5]. DTT assay is an indicative of

specificity of the reaction. NBD-Cl-adduct can be released from βTyr-297 after incubating with DTT [30, 31]. The mutants regained the activity indicating the release of NBD-Cl adducts from βTyr-297 [Fig 6]. The rate of inactivation was linearly dependant on NBD-Cl concentration and protection occurs at high concentrations of MgADP. All the mutants regained their phosphate binding activity when protected against NBD-Cl by MgADP [Fig 7].

Earlier studies established that mutagenesis combined with the use of the P_i protection assay against NBD-Cl inhibition, as well as the use of inhibitory analogs, enabled characterization of functional role(s) of residues suspected to be involved in P_i binding [36-38]. αD350R, αD350Q, αD350A mutants showed Pi binding where as αR376A mutant abrogated Pi binding in presence of wild type because of the loss of positive side chain of arginine residue [Fig 8]. Similarly, αG351R didn't show any Pi binding in presence of αR376D. However the introduction of arginine at α350 position compensated the loss of arginine at α376 position and regained the Pi binding activity. However, αD350R/αR376D showed partial gain in Pi binding [Fig 8]. The reasons for this might be the effect of charge and introduction of bulky groups. The growth on succinate and ATPase activities also supported the Pi protection assays.

Fluoroaluminate and fluoroscandium in combination with MgADP potently inhibit wild type *E. coli* ATP synthase [20-21, 36-37] and both are believed to mimic the chemical transition state. Transition state-like structures involving bound MgADP-AlF_4^- complex have been seen in catalytic sites in ATP synthase by x-ray crystallography [21]. It was observed from the fluoroaluminate and fluoroscandium experiments that there is a de-stabilization in transition state in αR376A, αG351R, αG351R/αR376D and αG351R/αR376A which was supported by Pi binding experiments [Fig 9]. The partial transition state stabilization is seen in the rest of the mutants, which is in agreement with Pi binding and oxidative phosphorylation. This shows that

there is a functional impairment in all the mutants. There is no loss of transition state stabilization in αD350Q that acts similar to wild type [Fig 9] .This may be due to the bulky nature of the amino group and its role in catalysis might be indirect.

From the results, we can conclude that the introduction of positive charged residue arginine (R) at αD350 position resulted in the catalysis of ATP synthase and thus played an important role in Pi binding, whereas the introduction of alanine (A) in αD350 is involved in partial transition state stabilization. The αD350Q mutant was inhibited completely by NBD-Cl and regaining the Pi binding activity just like the wild type. It also showed loss of transition state stabilization indicating that the introduction of a bulky group doesn't have any effect in Pi binding. The mutant αR376A abrogated the Pi binding and showed a destabilized transition state in fluoroaluminate and fluoroscandium experiments. This shows that αR376 is an important Pi binging residue that was already known [22]. The introduction of arginine in αD350 compensated the loss of arginine at α376 (αR376A) position. NBD-Cl showed 80-90% inhibition, Pi binding was completely regained and transition state stabilization was seen. This indicates that the introduction of positive charge in αD350 position compensated the loss of arginine at α376 .Thus, we can say that αD350R/αR376A plays an important role in Pi binding.

The mutant αD350R/αR376D didn't show much difference in Pi binding and also in transition state stabilization. The mutant's αG351R, αG351R/αR376A/D didn't show any significant difference. They showed partial inhibition with NBD-Cl and partial transition state stabilization by fluoroaluminate and fluoroscandium experiments. This indicates that αG351 may not be involved in Pi binding but may be involved in structural integrity of the ATP synthase.

Thus, we can accept the hypotheses that αD350 may be involved in Pi binding directly and is functionally important residue for maintaining structural integrity. This hypothesis was even supported by the compensatory effect of αD350. However, αG351 may not be involved in Pi binding directly but may be involved in structural integrity.

In the future, in order to confirm that αD350 plays an important role in Pi binding directly, we need to perform X-Ray crystal studies and determine the role played by the residues. The results shown were only from one set of membranes. So, in order to confirm the effect of mutations, assays need to be performed with another set of membranes. The effect of mutations on folding has to be determined through fluorescence studies.

REFERENCES

1. Slater EC. 1953. Mechanism of phosphorylation in the respiratory chain. *Nature* 172(4387):975-8.

2. Brodie AF, Gray CT. 1956. Activation of coupled oxidative phosphorylation in bacterial particulates by a soluble factor (s). *Biochim Biophys Acta* 19(2):384-6.

3. Penefsky HS, Pullman ME, Datta A, Racker E. 1960. Partial resolution of the enzymes catalyzing oxidative phosphorylation. II. Participation of a soluble adenosine tolphosphatase in oxidative phosphorylation. *J Biol Chem* 235:3330-6.

4. Mitchell P. 1961. Coupling of phosphorylation to electron and hydrogen transfer by a chemi-osmotic type of mechanism. *Nature* 191:144-8.

5. Weber J, Senior AE. 2003. ATP synthesis driven by proton transport in F1F0-ATP synthase. *FEBS Lett* 545(1):61-70.

6. Senior AE, Nadanaciva S, Weber J. 2002. The molecular mechanism of ATP synthesis by F1F0-ATP synthase. *Biochim Biophys Acta* 1553(3):188-211.

7. Noji H, Yoshida M. 2001. The rotary machine in the cell, ATP synthase. *J Biol Chem* 276(3):1665-8.

8. Leslie AG, Walker JE. 2000. Structural model of F1-ATPase and the implications for rotary catalysis. *Philos Trans R Soc Lond B Biol Sci* 355(1396):465-71.

9. Rosing J, Kayalar C, Boyer PD. 1977. Evidence for energy-dependent change in phosphate binding for mitochondrial oxidative phosphorylation based on measurements of medium and intermediate phosphate-water exchanges. *J Biol Chem* 252(8):2478-85.

10. Boyer PD. 1989. A perspective of the binding change mechanism for ATP synthesis. *FASEB J* 3(10):2164-78.

11. al-Shawi MK, Senior AE. 1992. Catalytic sites of Escherichia coli F1-ATPase. Characterization of unisite catalysis at varied pH. *Biochemistry* 31(3):878-85.

12. Weber J, Lee RS, Wilke-Mounts S, Grell E, Senior AE. 1993. Combined application of site-directed mutagenesis, 2-azido-ATP labeling, and lin-benzo-ATP binding to study the noncatalytic sites of Escherichia coli F1-ATPase. *J Biol Chem* 268(9):6241-7.

13. Ahmad Z, Senior AE. 2005. Identification of phosphate binding residues of Escherichia coli ATP synthase. *J Bioenerg Biomembr* 37(6):437-40.

14. Weber J, Bowman C, Wilke-Mounts S, Senior AE. 1995. alpha-Aspartate 261 is a key residue in noncatalytic sites of Escherichia coli F1-ATPase. *J Biol Chem* 270(36):21045-9.

15. al-Shawi MK, Parsonage D, Senior AE. 1989. Kinetic characterization of the unisite catalytic pathway of seven beta-subunit mutant F1-ATPases from Escherichia coli. *J Biol Chem* 264(26):15376-83.

16. Wise JG, Senior AE. 1985. Catalytic properties of the Escherichia coli proton adenosinetriphosphatase: evidence that nucleotide bound at noncatalytic sites is not involved in regulation of oxidative phosphorylation. *Biochemistry* 24(24):6949-54.

17. Orriss GL, Leslie AG, Braig K, Walker JE. 1998. Bovine F1-ATPase covalently inhibited with 4-chloro-7-nitrobenzofurazan: the structure provides further support for a rotary catalytic mechanism. *Structure* 6(7):831-7.

18. Perez JA, Greenfield AJ, Sutton R, Ferguson SJ. 1986. Characterisation of phosphate binding to mitochondrial and bacterial membrane-bound ATP synthase by studies of inhibition with 4-chloro-7-nitrobenzofurazan. *FEBS Lett* 198(1):113-8.

19. Menz RI, Walker JE, Leslie AG. 2001. Structure of bovine mitochondrial F(1)-ATPase with nucleotide bound to all three catalytic sites: implications for the mechanism of rotary catalysis. *Cell* 106(3):331-41.

20. Ahmad Z, Senior AE. 2004. Mutagenesis of residue betaArg-246 in the phosphate-binding subdomain of catalytic sites of Escherichia coli F1-ATPase. *J Biol Chem* 279(30):31505-13.

21. Ahmad Z, Senior AE. 2004. Role of betaAsn-243 in the phosphate-binding subdomain of catalytic sites of Escherichia coli F(1)-ATPase. *J Biol Chem* 279(44):46057-64.

22. Li W, Brudecki LE, Senior AE, Ahmad Z. 2009. Role of {alpha}-subunit VISIT-DG sequence residues Ser-347 and Gly-351 in the catalytic sites of Escherichia coli ATP synthase. *J Biol Chem* 284(16):10747-54.

23. Miller EM, Nickoloff JA. 1995. Escherichia coli electrotransformation. *Methods Mol Biol* 47:105-13.

24. Ausubel FM, Brent R, Kingston RE, Moore DD, Seidman JG, Smith JA, Struhl K. 1987. *Current Protocols in Molecular Biology*. John Wiley & Sons, NY.

25. Braman J, Papworth C, Greener A. 1996. Site-directed mutagenesis using double-stranded plasmid DNA templates. *Methods Mol Biol* 57:31-44.

26. Nelson M, McClelland M. 1992. Use of DNA methyltransferase/endonuclease enzyme combinations for megabase mapping of chromosomes. *Methods Enzymol* 216:279-303.

27. Senior AE, Langman L, Cox GB, Gibson F. 1983. Oxidative phosphorylation in Escherichia coli. Characterization of mutant strains in which F1-ATPase contains abnormal beta-subunits. *Biochem J* 210(2):395-403.

28. Senior AE, Latchney LR, Ferguson AM, Wise JG. 1984. Purification of F1-ATPase with impaired catalytic activity from partial revertants of Escherichia coli uncA mutant strains. *Arch Biochem Biophys* 228(1):49-53.

29. Taussky HH, Shorr E. 1953. A microcolorimetric method for the determination of inorganic phosphorus. *J Biol Chem* 202(2):675-85.

30. Ferguson SJ, Lloyd WJ, Lyons MH, Radda GK. 1975. The mitochondrial ATPase. Evidence for a single essential tyrosine residue. *Eur J Biochem* 54(1):117-26.

31. Ferguson SJ, Lloyd WJ, Radda GK. 1975. The mitochondrial ATPase. Selective modification of a nitrogen residue in the beta subunit. *Eur J Biochem* 54(1):127-33.

32. Ahmad Z, Senior AE. 2005. Involvement of ATP synthase residues alphaArg-376, betaArg-182, and betaLys-155 in Pi binding. *FEBS Lett* 579(2):523-8.

33. Braig K, Menz RI, Montgomery MG, Leslie AG, Walker JE. 2000. Structure of bovine mitochondrial F(1)-ATPase inhibited by Mg(2+) ADP and aluminium fluoride. *Structure* 8(6):567-73.

34. Penefsky HS. 2005. Pi binding by the F1-ATPase of beef heart mitochondria and of the Escherichia coli plasma membrane. *FEBS Lett* 579(10):2250-2.

35. Copley RR, Barton GJ. 1994. A structural analysis of phosphate and sulphate binding sites in proteins. Estimation of propensities for binding and conservation of phosphate binding sites. *J Mol Biol* 242(4):321-9.

36. Ahmad Z, Senior AE. 2005. Modulation of charge in the phosphate binding site of Escherichia coli ATP synthase. *J Biol Chem* 280(30):27981-9.

37. Ahmad Z, Senior AE. 2006. Inhibition of the ATPase activity of Escherichia coli ATP synthase by magnesium fluoride. *FEBS Lett* 580(2):517-20.

38. Brudecki LE, Grindstaff JJ, Ahmad Z. 2008. Role of alphaPhe-291 residue in the phosphate-binding subdomain of catalytic sites of Escherichia coli ATP synthase. *Arch Biochem Biophys* 471(2):168-75.

39. Weber J, Senior AE. 2000. ATP synthase: what we know about ATP hydrolysis and what we do not know about ATP synthesis. *Biochim Biophys Acta* 1458(2-3):300-9.

40. Nanomedicine Overview. 2010. National Institutes of Health. Division of Program Coordination, Planning, and Strategic Initiatives. Bethesda, Maryland, USA. Accessed Nov., 2010. http://nihroadmap.nih.gov/nanomedicine/

41. Whitesides, G. M. (2003) The 'Right' Size in Nanobiotechnology. *Nat Biotechnol* 21:1161-5.

42. Weber J. 2007. ATP synthase--the structure of the stator stalk. *Trends Biochem Sci* 32(2):53-6.

APPENDICES

APPENDIX A- Abbreviations

VISIT-DG- Valine-Isoleucine-Serine-Isoleucine-Threonine-Aspartate-Glutamate

ATP- Adenosine triphosphate

ADP- Adenosine diphosphate

Arg [R]- Arginine

Lys [L]- Lysine

Ser [S]- Serine

Gly [G]- Glycine

Asp [D]- Aspartate

Ala [A]- Alanine

Tyr- Tyrosine

AMP-PNP- Adenylyl imidodiphosphate

βTP- β triphosphate

βDP- β diphosphate

βE- β empty

NBD-Cl- 4-chloro-7-nitrobenzofurazan

MgADP- Magnesium adenosine diphosphate

AlF_4^-- Fluoroaluminate

TRIZMA- Tris [Hydroxyethyl] ethane

PAB- 4-aminobenzamidine

SDS- Sodium dodecyl sulphate

IPTG- Isopropyl-β-D-1- thio-galactopyranoside

X-Gal- 5-bromo-4-chloro-3-indolyl-beta-D-galactopyranoside

DTT-Dithiothreitol

NaF- Sodium fluoride

$Alcl_3$- Aluminum Chloride

$Sncl_3$- Scandium Chloride

T&S- Taussky and Shorr

O.D- Optical density

ATP_{cktl}- ATP cocktail

Mbr- Membrane

Inc-Incubate

APPENDIX B- Buffers and Reagents

50 mM Tris-SO_4 buffer

To 90 ml H_2O add

0.61 g Tris

Adjust pH to 8.0 with H_2SO_4

Bring to a final volume of 100 ml with H_2O

ATPase cocktail

In 150 ml H_2O add

10 ml 1 M Tris

0.8 ml 1M $MgCl_2$

5 ml 0.4 Na ATP (Adenosine 5'-triphosphate disodium salt)

Adjust pH to 8.5 with H_2SO_4

Bring to a final volume of 200 ml with H_2O

Freeze in plastic bottles at -20°C

10 % SDS

100 gm Sodium dodecyl sulfate

Bring to a final volume of 1000 ml with H_2O

T & S reagent / Taussky and Shorr reagent

Sol A: 1.2 g Ammonium molybdate ($(NH_4)_6Mo_7O_{24}\cdot 4H_2O$ in 9.8 ml 12 N H_2SO_4)

Sol B: 10 g Ferrous ammonium sulfate ($Fe(NH_4)_2(SO_4)_2\cdot 6H_2O$ in 70 ml H_2O)

Add sol A to sol B while stirring

Bring to a final volume of 100 ml with H_2O

Store at 4°C

STEM

To 700 ml H_2O add

100 ml 1 M TES

4.29 g Mg $(CH_3CO_2)_2 \cdot 4H_2O$

85.5 g sucrose

0.0951 g EGTA (Ethylene glycol-bis(2-aminoethylether)-N,N,N,N-tetraacetic acid)

5 g EACA (6-Ainocaproic acid6-Ainocaproic acid)

Adjust pH to 6.5 with NaOH

Bring to a final volume of 1000 ml with H_2O

Freeze in plastic bottles at -20°C

TES 50

To 700 ml H_2O add

50 ml 1 M TES

150 ml glycerol

5 g EACA (6-Ainocaproic acid6-Ainocaproic acid)

1 g PAB (4-Aminobenzamidine dihydrochloride)

Adjust pH to6.5 with NaOH

Bring to a final volume of 1000 ml with H_2O

Freeze in plastic bottles at -20°C

TES 5 + PAB

To 700 ml H_2O add

5 ml 1 M TES

150 ml glycerol

1 ml 0.5 M DTT (Dithiothreitol)

5 g EACA (6-Ainocaproic acid6-Ainocaproic acid)

1 g PAB (4-Aminobenzamidine dihydrochloride)

2.5 ml 0.2 M EDTA (Ethylenediaminetetraacetic acid disodium salt dihydrate)

Adjust pH to 6.5 with NaOH

Freeze in plastic bottles at -20°C

AET (Arginine Ent Thiamine)

To 60 ml H_2O add

0.617 g 2, 3 dihydroxy benzoic acid

16.86 g L-Arginine HCl

1 ml 20 mM Thiamine

Add just enough amount of NaOH to dissolve everything

Make final volume to 100 ml with H_2O

Filter sterile and store.

TE (Trace Elements)

To 80 ml H_2O

0.251 g Zinc Sulfate ($ZnSO_4.7H_2O$)

0.017 g Manganese Sulfate ($MnSO_4.H_2O$)

0.029 g Boric acid (H_3BO_3)

0.012 g Calcium Sulfate ($CaSO_4.2H_2O$)

0.037 g Calcium Chloride ($CaCl_2.2H_2O$)

0.049 g Ferric Chloride ($FeCl_3.6H_2O$)

Make final volume to 100 ml with H_2O.

Filter sterile and store.

ILV (Isoleucin-Valine)

To 95 ml H_2O add

0.394 g Isoleucine

0.352 g Valine

Make final volume to 100 ml with H_2O

Filter sterile

10x Reaction buffer

100 mM KCl

100 mM (NH4)2SO4

200 mM Tris-HCl (pH 8.8)

20 mM MgSO4

1% Triton® X-100

1 mg/ml nuclease-free bovine serum albumin (BSA)

Cell lysis solution

0.2M NaOH

1% SDS

Cell resuspension solution

50mM Tris-HCl (pH 7.5)

10mM EDTA

100µg/ml RNase A

Column wash solution

162.8mM Potassium acetate

22.6mM Tris-HCl (pH 7.5)

0.109mM EDTA (pH 8.0)

Neutralization solution

4.09M Guanidine hydrochloride

0.759M Potassium acetate

2.12M Glacial acetic acid

Adjust the final pH to approximately 4.2.

APPENDIX C- Culture Media and Plates

LB liquid medium:

12.5 g of LB broth powder

Add H_2O to bring to 500 ml

Autoclave for 30 minutes

Cool the media to ~50°C

Add 500 µl of 100 mg/ml Ampicillin

Minimal Glucose:

To 400 ml H_2O add

5.225 g Potassium Phosphate Dibasic Trihydrate (K_2HPO_4)

2.40 g Sodium Phosphate Monobasic (NaH_2PO_4)

0.99 g Ammonium Sulfate ($(NH_4)_2SO_4$)

Autoclave for 30 min, cool it and add the following additions

10 ml Uracil

10 ml 27 % Glucose

5 ml ILV (isoleucin-valine)

0.5 ml TE (trace elements)

0.5 ml 1 M Magnesium Sulfate ($MgSO_4$)

0.5 ml AET (Arginine Ent Thiamine)

0.5 ml 100 mg/ml Ampicillin

0.312 ml 4X LB

LB-Agar plate with Ampicillin:

12.5g of LB broth powder

7.5g of Agar

Bring to a final volume of 500 ml

Autoclave for 30 minutes

Cool the media to ~50°C

Add 500 µl of 100 mg/ml Ampicillin

Pour into sterile plates

NZY^{+} broth:

To 900 ml of deionized water, add

10 g of NZ amine (casein hydrolysate)

5 g of Yeast extract

5 g of NaCl

Adjust to pH 7.5 using NaOH and make the final volume to 1 liter.

Autoclave and add the following filer-sterilized supplements prior to use:

12.5 ml of 1 M MgCl2

12.5 ml of 1 M MgSO4

and 10 ml of 2M glucose or 20 ml of 20% (w/v) glucose.

VITA

SNEHA REDDY JONNALAGADDA

Personal Data:	Date of Birth: August 13, 1984. Place of Birth: Miryalguda, Andhra Pradesh, India. Marital Status: Married
Education:	B.Tech in Biotechnology, JNTU, A.P, India, 2007 M.S. in Biology, East Tennessee State University, Johnson City, TN, 2011.
Professional Experience:	Graduate Assistant, East Tennessee State University, College of Arts and Sciences, 2009-2011.
Presentations:	Sneha R. Jonnalagadda (2010). "Role of α- subunit VISIT-DG sequence residue Asp-350 in the catalytic site of *Escherichia coli* ATP Synthase". Seminar and Presentation at Appalachian student research forum, East Tennessee State University, Johnson City, TN.